

AD-A090 716

NAVAL OCEAN SYSTEMS CENTER SAN DIEGO CA

F/G 20/14

EFFECTS OF IONOSPHERIC REFLECTION HEIGHT AND GROUND CONDUCTIVITY--ETC(U)

JUN 80 W.F. MOLER, R A PAPPERT

DNA-MIPR-80-563

UNCLASSIFIED

NOSC/TR-561

NL

1 OF 1
AD-A090 716

NOSC

0

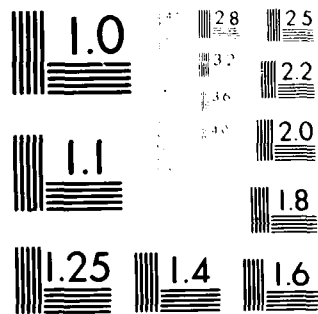
END

DATE

FILED

11-80

DTIC



MICROCOPY RESOLUTION TEST CHART
NATIONAL BUREAU OF STANDARDS-1963-A

12

LEVEL III

NOSC

NOSC TR 561

AD A090716

46/S99QAXH

115-751

NOSC TR 561

Technical Report 561

EFFECTS OF IONOSPHERIC REFLECTION HEIGHT AND GROUND CONDUCTIVITY ON EARTH-IONOSPHERE WAVEGUIDE MODE AND GROUND-WAVE ATTENUATION RATES.

10/DNA-MIT-100-001

12/231

10/W.F./Moler
R.A./Pappert

11/June 1980

DTIC
ELECTE
S OCT 23 1980 D

9/Interim Report October 1979-April 1980

This work sponsored by the
DEFENSE NUCLEAR AGENCY under Subtask
S99QAXHBO42 and Work Unit 25

F

14/1150/11561

Approved for public release; distribution unlimited

NAVAL OCEAN SYSTEMS CENTER
SAN DIEGO, CALIFORNIA 92152

DOC FILE COPY

80 10 22 005



NAVAL OCEAN SYSTEMS CENTER, SAN DIEGO, CA 92152

AN ACTIVITY OF THE NAVAL MATERIAL COMMAND

SL GUILLE, CAPT, USN

Commander

HL BLOOD

Technical Director

ADMINISTRATIVE INFORMATION

This work, sponsored by the Defense Nuclear Agency under subtask code S99QAXHB042 and work unit 25, was performed by the Nuclear Effects Branch during the period 1 October 1979 through 1 April 1980. The report was approved for publication June 1980.

Released by
JH Richter, Head
EM Propagation Division

Under authority of
JD Hightower, Head
Environmental Sciences
Department

UNCLASSIFIED

SECURITY CLASSIFICATION OF THIS PAGE (When Data Entered)

REPORT DOCUMENTATION PAGE		READ INSTRUCTIONS BEFORE COMPLETING FORM
1. REPORT NUMBER NOSC Technical Report 561	2. GOVT ACCESSION NO. AD-4090716	3. RECIPIENT'S CATALOG NUMBER
4. TITLE (and Subtitle) EFFECTS OF IONOSPHERIC REFLECTION HEIGHT AND GROUND CONDUCTIVITY ON EARTH - IONOSPHERE WAVEGUIDE MODE AND GROUND-WAVE ATTENUATION RATES		5. TYPE OF REPORT & PERIOD COVERED Interim: Oct 79 - Apr 80
7. AUTHOR(s) WF Moler RA Pappert		6. PERFORMING ORG. REPORT NUMBER
9. PERFORMING ORGANIZATION NAME AND ADDRESS Naval Ocean Systems Center San Diego, CA 92152		8. CONTRACT OR GRANT NUMBER(s) DNA MIPR 80-563
11. CONTROLLING OFFICE NAME AND ADDRESS Defense Nuclear Agency Washington, D.C. 20350		10. PROGRAM ELEMENT, PROJECT, TASK AREA & WORK UNIT NUMBERS 6-27-04 H, S99QAXHB042, 532-MP2025, ELFWLF
14. MONITORING AGENCY NAME & ADDRESS (if different from Controlling Office)		12. REPORT DATE June 1980
		13. NUMBER OF PAGES 27
		15. SECURITY CLASS. (of this report) Unclassified
		18a. DECLASSIFICATION/DOWNGRADING SCHEDULE
16. DISTRIBUTION STATEMENT (of this Report) Approved for public release; distribution unlimited		
17. DISTRIBUTION STATEMENT (of the abstract entered in Block 20, if different from Report)		
18. SUPPLEMENTARY NOTES		
19. KEY WORDS (Continue on reverse side if necessary and identify by block number) EM propagation Earth-ionosphere waveguide Ground wave		
20. ABSTRACT (Continue on reverse side if necessary and identify by block number) A surviving ground-wave signal has previously been assumed to represent the minimum expected for vlf and lf systems operating in a severely disturbed environment. The authors show that for propagation over poorly conducting soil and under a depressed ionosphere, path losses may markedly exceed those predicted by the normal ground-wave attenuation rates. This is shown to be caused by the invasion of the ionosphere into the presupposed free-space region of the diffraction mode (ground-wave) "dust." Because of inherent uncertainties in the ground-wave model for some propagation conditions, the authors recommend that estimates of system performance in severe environments be based on earth-ionosphere waveguide mode computational models. ←		

DD FORM 1 JAN 73 1473

EDITION OF 1 NOV 65 IS OBSOLETE
S/N 0102-LF-014-6601

UNCLASSIFIED

SECURITY CLASSIFICATION OF THIS PAGE (When Data Entered)

UNCLASSIFIED

SECURITY CLASSIFICATION OF THIS PAGE (When Data Entered)

Accession For	
CRA&I	<input checked="checked" type="checkbox"/>
CSB	<input type="checkbox"/>
Command	<input type="checkbox"/>
Function	
Availability Codes	
Avail and/or	
Dist	Special
A	

UNCLASSIFIED

SECURITY CLASSIFICATION OF THIS PAGE(When Data Entered)

CONTENTS

1. INTRODUCTION AND BACKGROUND . . .	page 4
2. THE GROUND WAVE . . .	6
2.1 Ground-Wave Attenuation . . .	12
2.2 Waveguide Mode Attenuation . . .	12
3. DISCUSSION OF RESULTS . . .	19
3.1 Comparison of Waveguide and Ground Wave . . .	19
4. CONCLUSIONS AND RECOMMENDATIONS . . .	26
REFERENCES . . .	27

FIGURES

- 1 Locus of reflection height H' and ground conductivity σ combinations which produce a principal TM waveguide mode attenuation rate α (WG) equal to the principal diffraction (ground-wave) mode attenuation rate α (GW) at 20 kHz . . . page 7
- 2 Electron collision frequency ν_e profile and electron density profiles consistent with ionospheric conductivity profiles given by $\omega_r(h) = 2.5 \times 10^5 \exp [\beta(h-H')] s^{-1}$ where $\beta = 0.2515 \text{ km}^{-1}$. . . 8
- 3 Track width as a function of frequency of the first three diffraction modes for propagation over a standard earth and perfectly reflecting ground . . . 10
- 4 Track width of the zero-order diffraction mode as a function of frequency and of ground conductivity σ . . . 11
- 5a-d Principal ground-wave mode attenuation rate as a function of ground conductivity for 10, 20, 40, and 60-kHz propagation. The solid curve is the attenuation resulting from ground absorption, the dashed curve is for attenuation resulting from leakage, and the broken curve shows the total attenuation . . . 13
- 6a-d Attenuation rate of the principal waveguide mode resulting from ground absorption (solid curve) and resulting from ionospheric absorption (dashed curve) as a function of ground conductivity for a number of reflection heights H' . The broken curve is the ground-wave attenuation as a function of surface conductivity . . . 15
- 7a-g Attenuation rate of the principal waveguide mode as a function of frequency for a number of reflection heights H' and for the ground conductivity σ specified on each figure. The ground-wave attenuation rate (curve GW) and the attenuation rate of a mode characterized by eigenangles equal to the complex Brewster angle (curve θ_B) are also shown for each ground conductivity . . . 20
- 8 Combinations of reflection height H' and surface conductivity σ which produce a principal TM waveguide mode attenuation rate equal to the ground-wave attenuation rate. For those combinations of H' and σ lying above each of the frequency curves, the TM waveguide mode attenuation is less than the ground-wave attenuation rate for that frequency and ground conductivity. For combinations below the curve, the TM mode attenuation rate is greater than the ground-wave attenuation rate . . . 25

OBJECTIVE

Determine whether the ground-wave signal for vlf and lf radio systems represents the minimal expected field strength under severely disturbed ionospheres.

RESULTS

Path losses can markedly exceed those predicted by normal ground-wave attenuation rates for propagation under simultaneously occurring conditions of depressed ionospheres and poorly conducting ground. When these conditions apply, the safest way to evaluate the vlf and lf system performance is by use of waveguide mode theory rather than by wave-hop or ground-wave techniques.

RECOMMENDATION

Because of the possible errors and misconceptions which may arise from using the ground-wave computation for estimating lf coverage in severely disturbed environments, a complete propagation analysis of coverage should be performed by means of numerical methods based on waveguide mode theory.

1. INTRODUCTION AND BACKGROUND

Much effort has been expended during the past few years in developing survivable communications for control of the strategic forces by the NCA and CINCS under nuclear warfare conditions. Both the Navy and the Air Force have developed airborne and fixed ground-station transmitters which radiate in the vlf and lf (10^4 – 10^5 Hz) radio bands to provide assured one-way communications from the command authorities to the strategic forces. The reliance on long-wave systems arose because practical transmitters and powers can provide near-global (or at least very-long-range) one-way assured communications. In addition, long-wave communications were considered to be much less vulnerable to disruption by the effects of nuclear detonations in the atmosphere than long-range hf communications. Radio measurements made during the 1962 high-altitude tests in the Pacific confirmed that long-wave systems did indeed suffer less severe propagation effects than hf systems, but the effects were much more severe than had been anticipated. Subsequently, researchers were able to show that, if positive and negative ions were included in the vlf and lf propagation models, the theoretical predictions were in line with observations made during the high-altitude nuclear tests.

A working group was organized by the Defense Nuclear Agency (DNA) at the RAND Corporation in November 1963 to study the effects of nuclear environments on lf propagation. Although details of the chemistry were not well known, it became apparent to the group that nuclear perturbation of the atmosphere below the normal D-region could drastically reduce lf (and vlf) sky-wave propagation. The major conclusion of the working group was: "In any event, it appears basically sound, in order to provide invulnerability to nuclear burst-produced propagation effects, to design lf systems on the basis of the surviving ground wave signal and normally expected noise background."¹ The remarks preceding the above quotation are essentially a distillation of the introduction and background from reference 1 and serve well as background material for this report.

In part D of reference 1, Crain illustrates how one may calculate the signal amplitude reduction for a given path length and for several radio frequencies if the sky wave were completely absorbed by a severe nuclear environment. That is, the signal reduction represents the difference between signal levels in a normal quiescent environment and that produced by a ground wave only. In presenting this approach, Crain points out that it is approximate and that path losses are apt to be greater than given by the simple sky-wave–ground-wave difference in signal level; that losses increase with decreasing radio frequency and with increasing nuclear perturbation. Crain assumed "typical" earth conductivity and typically normal day and night ionospheres.

Crain's ground-wave attenuation rates were calculated for free-space conditions above a conducting earth. Johler² examined ground-wave propagation in a uniformly ionized atmosphere and found that if the ionization were sufficiently intense, ground-wave attenuation

¹ Crain, C.M., An Overview Discussion of Propagation Effects of Nuclear Environments on VLF-LF Communications Systems, RAND Corporation Report to Defense Nuclear Agency, DNA 3778T, 31 August 1975.

² Johler, J.R., Ground Wave Propagation in a Normal and an Ionized Atmosphere, ESSA Research Laboratories Report ERL 121-ITS 85, July 1969.

would be increased. In a subsequent report, Johler³ again examined the effects of nuclear-produced ionization on ground-wave propagation but with a more realistic ionization profile, one which had a steep gradient of ionization with altitude. He again found sizeable increases in ground-wave attenuation for large nuclear contamination. Using Johler's approach³, it certainly would be possible to modify the path loss estimation method of Crain¹ to take into account ground-level ionization for appropriate nuclear fallout models. However, in this report we examine some other effects which increase the ground-wave attenuation of long waves. It has long been recognized that combinations of low ground conductivity and low ionospheric heights lead to very large attenuations in the earth-ionosphere waveguide. Pappert⁴ analyzed the effects of ground conductivity variations on quasi-TE and quasi-TM waveguide modes excited by both vertical and horizontal dipoles. Calculations for ground conductivities ranging from 10 to 10^{-5} S/m showed that excitation factors drop rapidly with decreasing conductivity and that the dominant TM mode attenuation rates for 10^{-5} S/m ground conductivity were the order of 15–20 dB/Mm as opposed to a few dB/Mm for 10^{-3} S/m ground. The increased attenuation was much more severe in the daytime than at night. Field et al⁵ demonstrated that theoretical computations of long-wave (elf/vlf/lf) path losses over ice during PCAs were consistent with experimental measurements of vlf transmissions over propagation paths crossing the Greenland ice cap. They also demonstrated that path losses measured in a scaled physical model waveguide gave qualitative substantiation of both the theory and vlf transmission measurements. Most important, they conclusively demonstrated that ionospheric depression over low conductivity ground (ice) produces path losses far in excess of those produced by the same ionospheric depression over sea water.

Westerlund et al⁶ found that a depressed polar ionosphere from a proton precipitation event caused extreme attenuation of vlf waves passing over the Greenland ice cap. In a subsequent paper, Westerlund and Reder⁷ demonstrated that the high attenuation of TM modes over ice is a function of ionospheric height, surface conductivity, and the dielectric constant of the ice. They also show that there is always a TM mode with eigenangles near the Brewster angle for conductivity less than about 10^{-4} S/m. They found good agreement between the theoretical models (using the NOSC waveguide program) and radio measurements.

-
3. Johler, J.R. . Atmospheric Nuclear Disturbances with Respect to the Ground Wave, ESSA Research Laboratories Technical Memorandum, ERLTM-ITS 217, March 1970.
 4. Pappert, R.A., Effects of Elevation and Ground Conductivity on Horizontal Dipole Excitation of the Earth-Ionosphere Waveguide, Radio Science, vol 5, pp 579–590, March 1980.
 5. Field, E.C., C. Greifinger, and K. Schwartz, Transpolar Propagation of Long Radio Waves, R-683-DASA, DASA 2621, RAND Corporation, March 1971.
 6. Westerlund, S., F.H. Reder, and C. Abom, Effects of Polar Cap Absorption Events on VLF Transmissions, Planetary and Space Science, 17, pp 1329–1374. 1969.
 7. Westerlund, S., and F.H. Reder, VLF Radio Signals Propagating over the Greenland Ice-Sheet, Journal of Atmospheric and Terrestrial Physics, vol 35, pp 1475–1491, 1973.

In the following sections, we look more closely at the assumption that a surviving ground wave provides the minimum expected signal in a severely disturbed environment. We briefly discuss the ground-wave model and indicate weaknesses in the model for real environments. We compare diffraction mode and waveguide mode attenuation mechanisms as a function of ground conductivity, ionospheric height, and frequency. Curves showing total principal mode attenuation rates as a function of ionospheric height, radio frequency, and ground conductivity are compared with ground-wave attenuation rates to indicate the environmental conditions for which the ground wave represents a reasonable, an unreasonably low, or an unreasonably high estimate of the surviving signal in a disturbed environment.

2. THE GROUND WAVE

The contribution of ground-wave components to the total field is accounted for by both the waveguide mode and wave-hop theories of EM wave propagation in the earth-ionosphere waveguide. The mode theory includes all propagating field components within a set of self-consistent resonant modes; the ground wave is included implicitly. The wave-hop theory considers the total field at some position in the guide to be the sum of contributions arriving along rays connecting transmitter and receiver via (1) reflections off the earth and ionosphere and (2) the ground-wave field. The ground wave makes an explicit contribution and is calculated separately. It follows from the wave-hop theory that, if the ionosphere becomes so lossy that sky-wave contributions to the field are negligible, the ground-wave field would remain as the minimum expected signal. It should also follow that, under the same lossy conditions, fields calculated by using waveguide mode theory would also approach a minimum at the ground-wave signal level. That these assumptions can be incorrect, particularly under conditions of low ground conductivity, is evidenced by figure 1.

The curve in figure 1 is the locus of "reflection height" (H') and ground conductivity (σ) combinations which produce a waveguide mode attenuation rate at 20 kHz equal to the ground-wave attenuation rate for the same ground conductivity. All combinations of H' and σ below the curve produce waveguide attenuation rates greater than the ground-wave rate; all above the curve produce waveguide attenuation rates less than the ground-wave attenuation rate. The attenuation rates considered were for the principal waveguide and ground-wave modes and represent the total field attenuation rates well beyond the horizon.

The waveguide mode parameters here and throughout this report are for ionospheric profiles which are exponential in terms of the conductivity parameter ω_r where:

$$\omega_r(h) = \frac{\omega_p^2(h)}{\nu(h)} = 2.5 \times 10^5 \exp [\beta (h-H')]^{-1}, \quad (1)$$

as given by Wait and Spies.⁸ The circular plasma frequency ω_p is proportional to the square root of the electron density and ν is the electron-neutral collision frequency. The scale height β is in inverse kilometers; the altitude h and the "reflection height" H' are in kilometers. For all calculations, $\beta = 0.2515 \text{ km}^{-1}$, taken to be representative of the weak conductivity gradients associated with the more lossy disturbed environments. The electron density profiles for several H' 's, along with the assumed electron collision frequency profile, are shown in figure 2.

⁸ Wait, J.R., and K.P. Spies, Characteristics of the Earth-Ionosphere Waveguide for VLF Radio Waves, US Dept of Commerce, National Bureau of Standards, Technical Note 300.

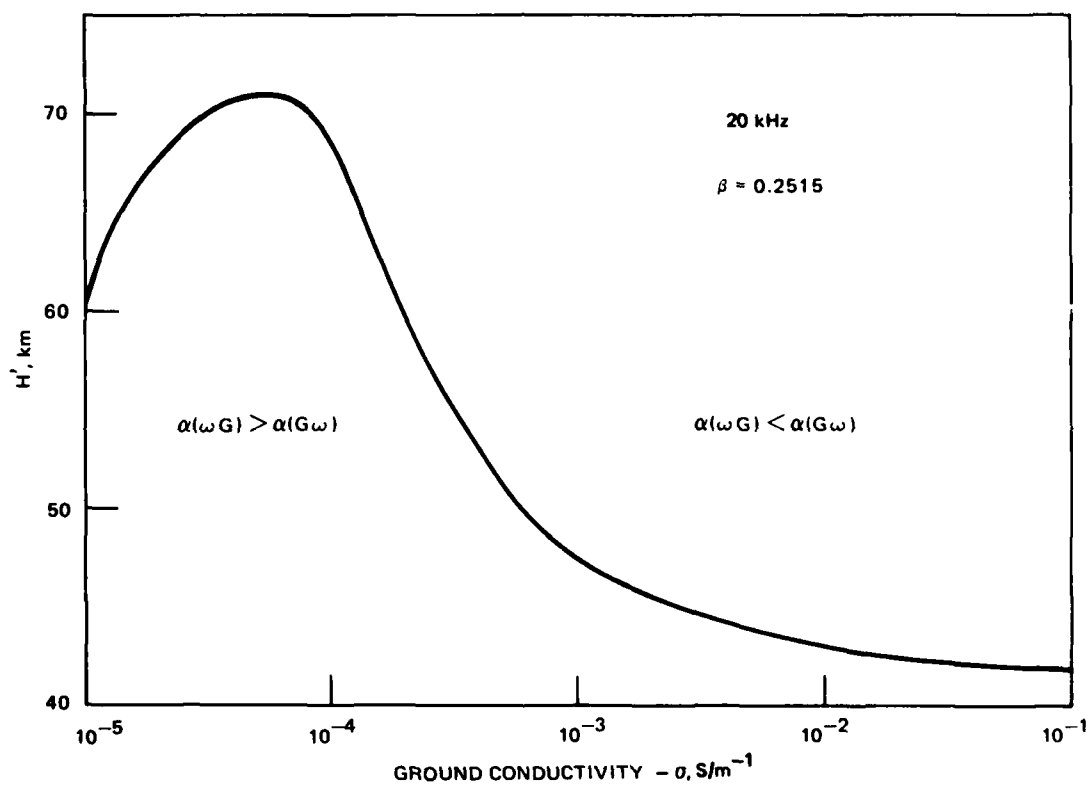


Figure 1. Locus of reflection height H' and ground conductivity σ combinations which produce a principal TM waveguide mode attenuation rate $\alpha(\text{WG})$ equal to the principal diffraction (ground-wave) attenuation rate $\alpha(\text{GW})$ at 20 kHz.

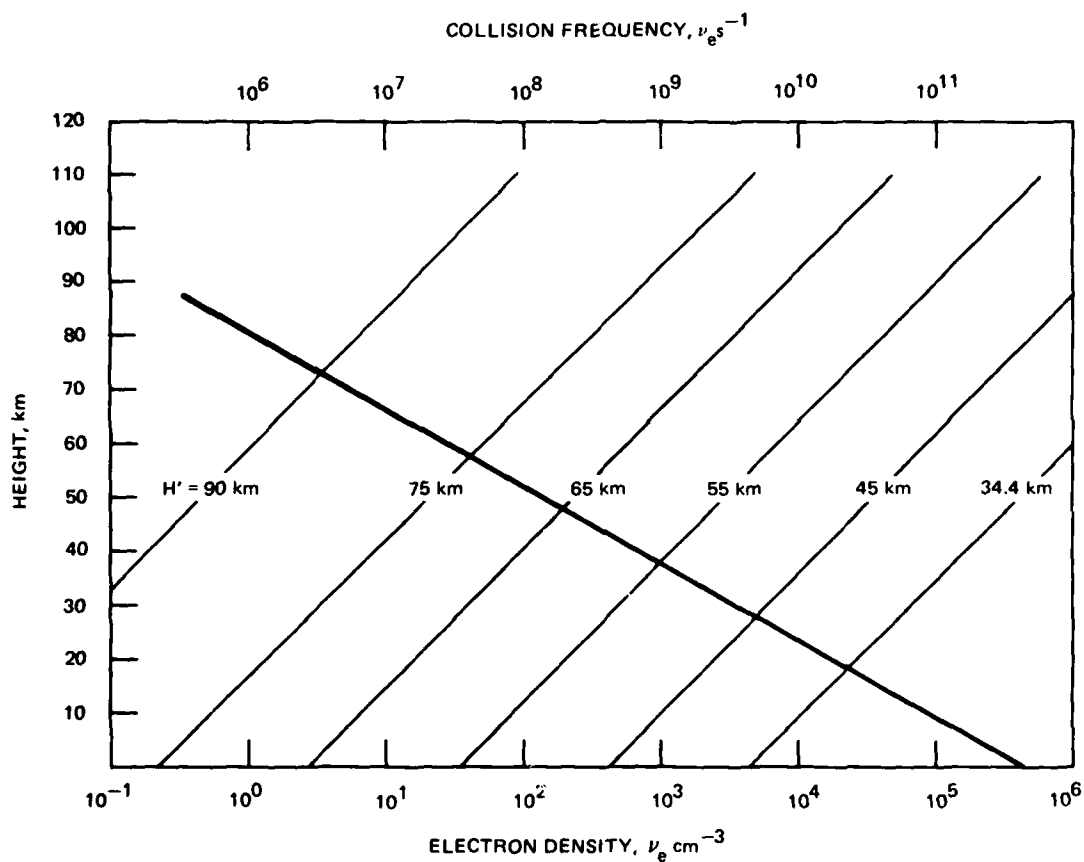


Figure 2. Electron collision frequency ν_e profile and electron density profiles consistent with ionospheric conductivity profiles given by $\omega_r(h) = 2.5 \times 10^5 \exp [\beta(h - H')] \text{ s}^{-1}$ where $\beta = 0.2515 \text{ km}^{-1}$.

One can better understand the discrepancy between earth-ionosphere waveguide and ground-wave computations of fields by examining the ground-wave model. For computation, the physical model of a spherical, finitely conductive earth surrounded by free space can be replaced by a planar earth of the same conductivity under a continuous refractive atmosphere. The gradient of refractive index is such that a horizontally launched ray has an upward curvature equal to the earth's curvature. The model is identical to that often used for earth-ionosphere waveguides for the free-space region below the ionosphere except that for the diffraction model the free-space region is infinite. It can be shown (Budden⁹) that, for certain complex angles of wave normals, upgoing waves are converted by an apparent reflection process into downgoing waves. At some angles of incidence, the downgoing waves are reflected from the earth and become indistinguishable from the original upgoing waves. These are, of course, the conditions for a set of self-consistent waveguide modes.

Near the ground, then, the diffraction modes consist of both upgoing and downgoing waves consistent with the modal condition. Yet at high altitudes only upgoing waves are allowed. This implies that something akin to reflection takes place at an intermediate height. The phase integral method, sometimes used as a first approximation for determining the modal solutions, involves the concept of a "complex reflection height", Z_0 . Booker and Walkinshaw¹⁰ have called the real part of Z_0 the "track width". The track width or, equivalently, "duct height" gives some physical feel for the depth of free space above the ground required to satisfy the diffraction field computational model. Figure 3 shows the track width as a function of frequency for the zero, first, and second diffraction modes for a standard earth and perfectly reflecting ground.

For ground of finite conductivity, changes in earth reflectivity modify the modal conditions and consequently the track width. Figure 4 shows the track width for the zero-order mode as a function of radio frequency for ground conductivities ranging from 10^{-1} S/m to 10^{-5} S/m. The track widths for $\sigma = 10^{-1}$ S/m are nearly identical to those shown by the $n = 0$ curve of figure 3.

If the concept of "track width" has any real physical significance, it is clear that at frequencies below about 25 kHz, daytime ionospheres encroach on the free-space region required by the ground-wave model for other than the zero-order mode (figure 3). It is equally clear (figure 3) that for conductivities less than 10^{-3} S/m it takes but little ionospheric depression below normal to modify the refractivity of the ground-wave "duct" of the zero-order mode. The implication of these arguments is that, under conditions leading to complete loss of sky waves, the conditions assumed for the ground-wave computation are likely not satisfied. Thus the assumption that the ground-wave field represents the minimum possible signal may be incorrect for certain combinations of radio frequency, ground conductivity, and ionospheric height.

9. Budden, K.G., The Waveguide Mode Theory of Wave Propagation, Logos Press, London, 1961.
10. Booker, H.G., and W. Walkinshaw, The Mode Theory of Tropospheric Refraction and its Relation to Wave-Guides and Diffraction, in Report: Meteorological Factors in Radio Wave Propagation, pp 80-127, London, Physical Society, 1946.

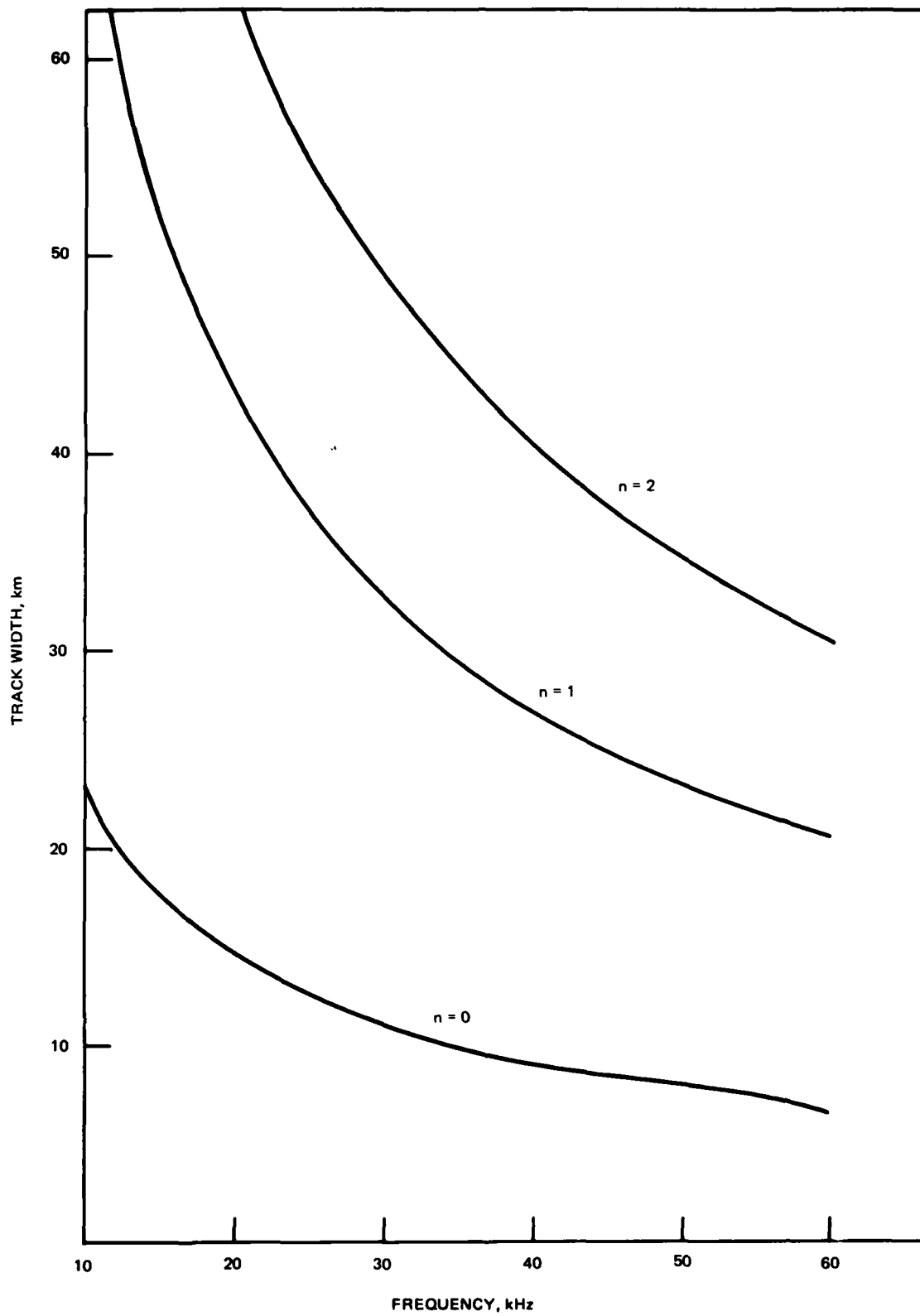


Figure 3. Track width as a function of frequency of the first three diffraction modes for propagation over a standard earth and perfectly reflecting ground.

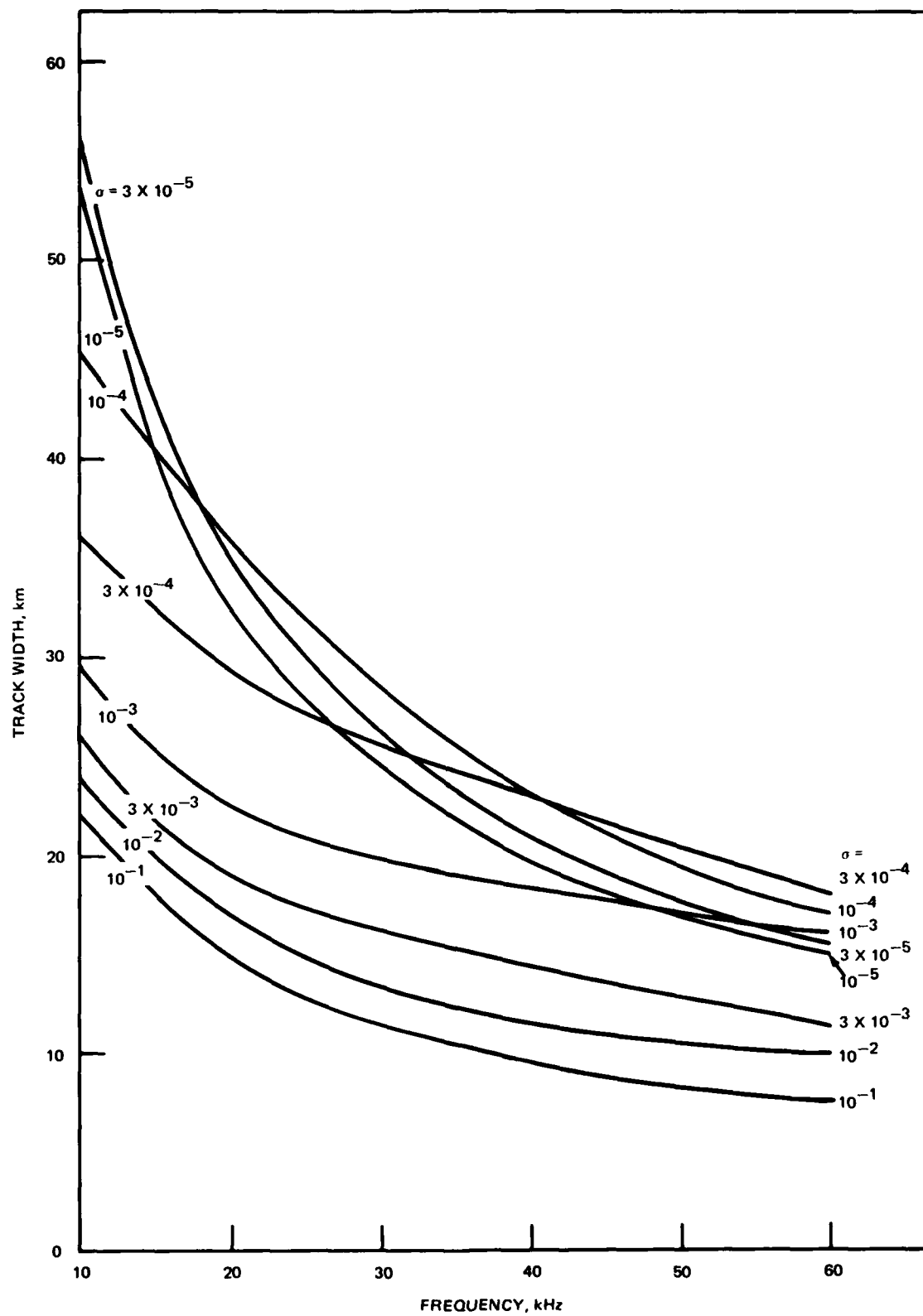


Figure 4. Track width of the zero-order diffraction mode as a function of frequency and of ground conductivity σ .

2.1 GROUND-WAVE ATTENUATION

Ground-wave fields lose energy by absorption in the earth and by leakage away into space. The total ground-wave attenuation rate can be calculated from its functional relationship with the diffraction mode eigenangle. Alternatively, it can be calculated directly from the field components at and above the earth's surface. Figures 5a-d show the attenuations due to ground absorption and to leakage, as well as their sum as a function of ground conductivity for 10-kHz, 20-kHz, 40-kHz, and 60-kHz ground waves, as calculated from the field components by taking the height of the guide equal to the track width.

The curves of attenuation due to ground absorption all show a steady increase with decreasing ground conductivity until they reach a broad maximum about some particular value of conductivity. At 20 kHz (figure 5b), attenuation by ground absorption is less than 1 dB/Mm at 10^{-1} S/m and increases to nearly 12 dB/Mm at 8×10^{-5} S/m before falling off to 9 dB/Mm at 10^{-5} S/m. At the same time, the attenuations resulting from leakage away from the earth show broad minima where the ground absorption losses maximize. In general, the leakage losses are the greater part of the total ground-wave attenuation except within a frequency-dependent band of surface conductivities. We will see later that the bulges of maximum ground absorption occur when the diffraction mode eigenangle is near the Brewster angle.

2.2 WAVEGUIDE MODE ATTENUATION

Waves propagating in the earth-ionosphere waveguide are attenuated by ohmic "heating" of the ground and of the lower ionosphere, and by leakage out of the guide along the geomagnetic field lines. Leakage losses are negligibly small during midday or when the ionosphere is overionized and depressed. Figures 6a-d show attenuation due to ground and ionospheric heating losses for the principal waveguide mode as a function of ground conductivity for several ionospheric heights (H') at 10, 20, 40, and 60 kHz, respectively. The total ground-wave attenuation rate is also included in each of the figures.

There are some striking differences in the attenuation due to ground heating between the ground-wave and waveguide modes. For both models, the attenuation from ground absorption has a broad maximum centered about those conductivities where the waveguide and diffraction mode eigenangles approach the surface complex Brewster angle. However, the waveguide modal eigenangles approach the Brewster angles at somewhat lower conductivities than do the diffraction mode eigenangles, particularly at the lower frequencies. The most important difference obviously results from the presence of an upper boundary of the waveguide. Lowering the ionosphere not only increases ionospheric absorption, but also greatly increases ground absorption. At the lower conductivities, even if the assumption were true that sky-wave absorption is identically equal to the ground-wave leakage losses, the enhanced ground losses under the depressed-ionosphere can materially exceed ground-wave surface absorption. In the next section we will, within the constraints of the model ionosphere show the conditions under which waveguide attenuation rates will exceed ground-wave attenuation rates.

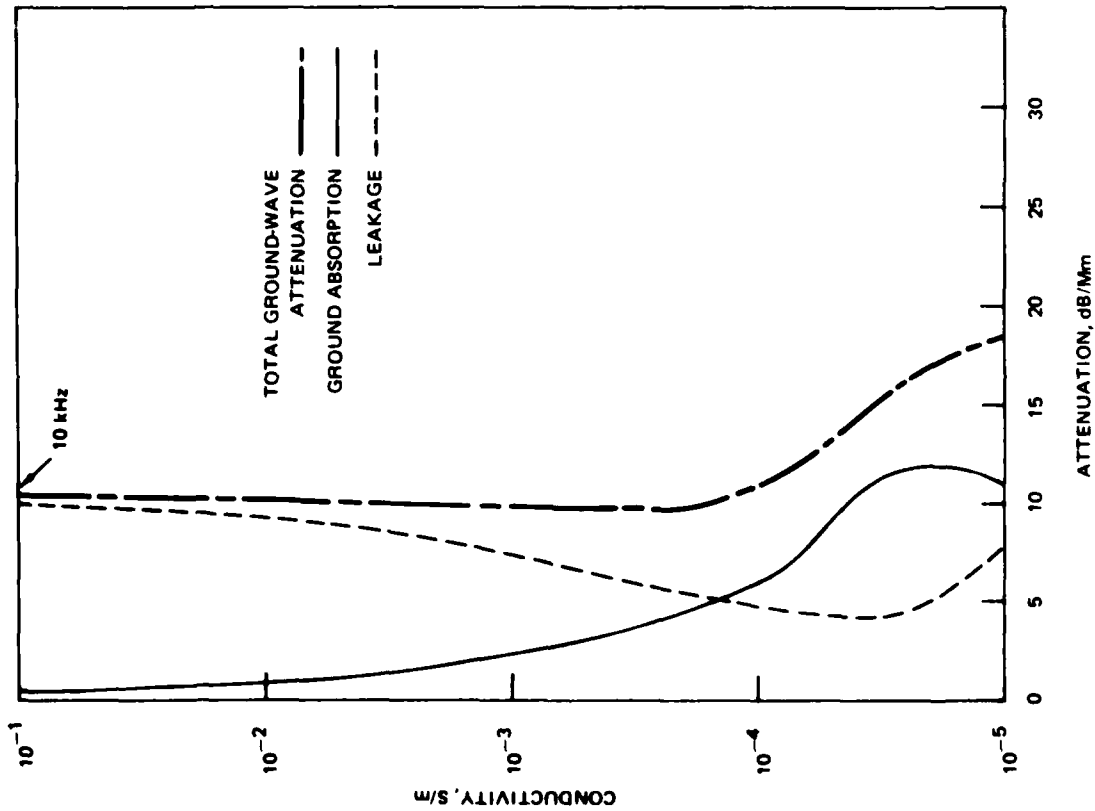


FIGURE 5a

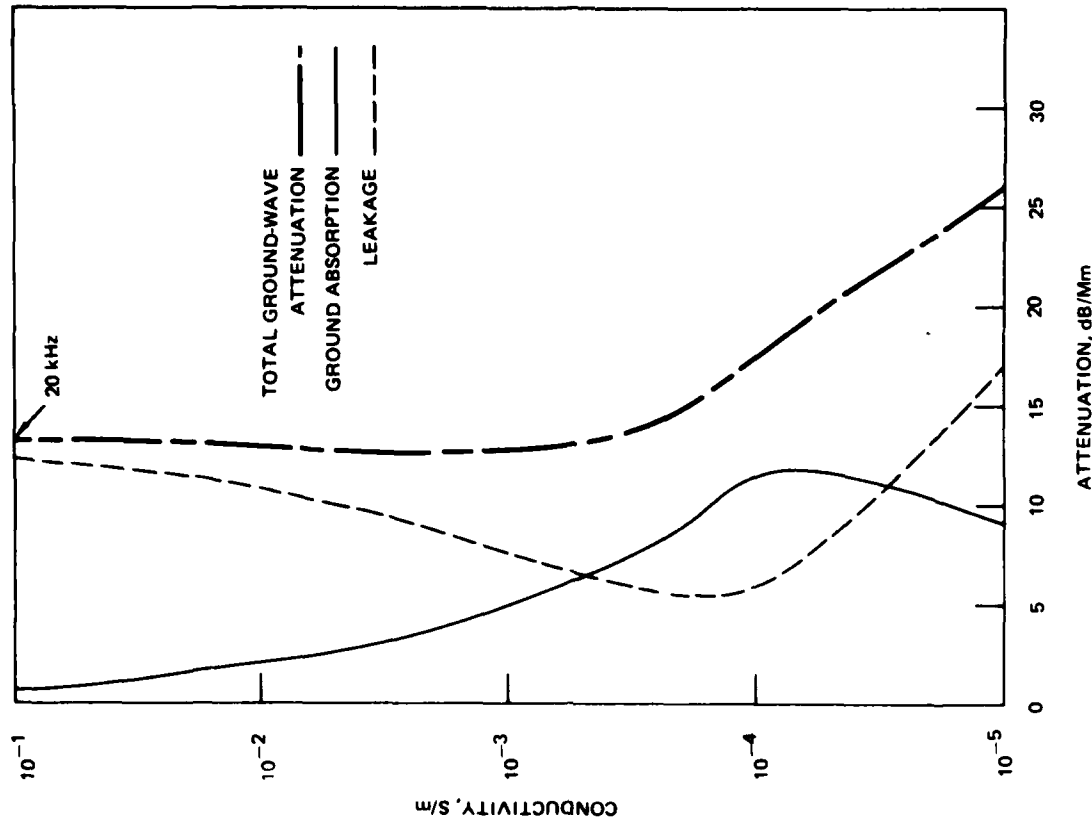


FIGURE 5b

Figure 5 a-d. Principal ground-wave mode attenuation rate as a function of ground conductivity for 10, 20, 40, and 60-kHz propagation. The solid curve is the attenuation resulting from ground absorption, the dashed curve is for attenuation resulting from leakage, and the broken curve shows the total attenuation.

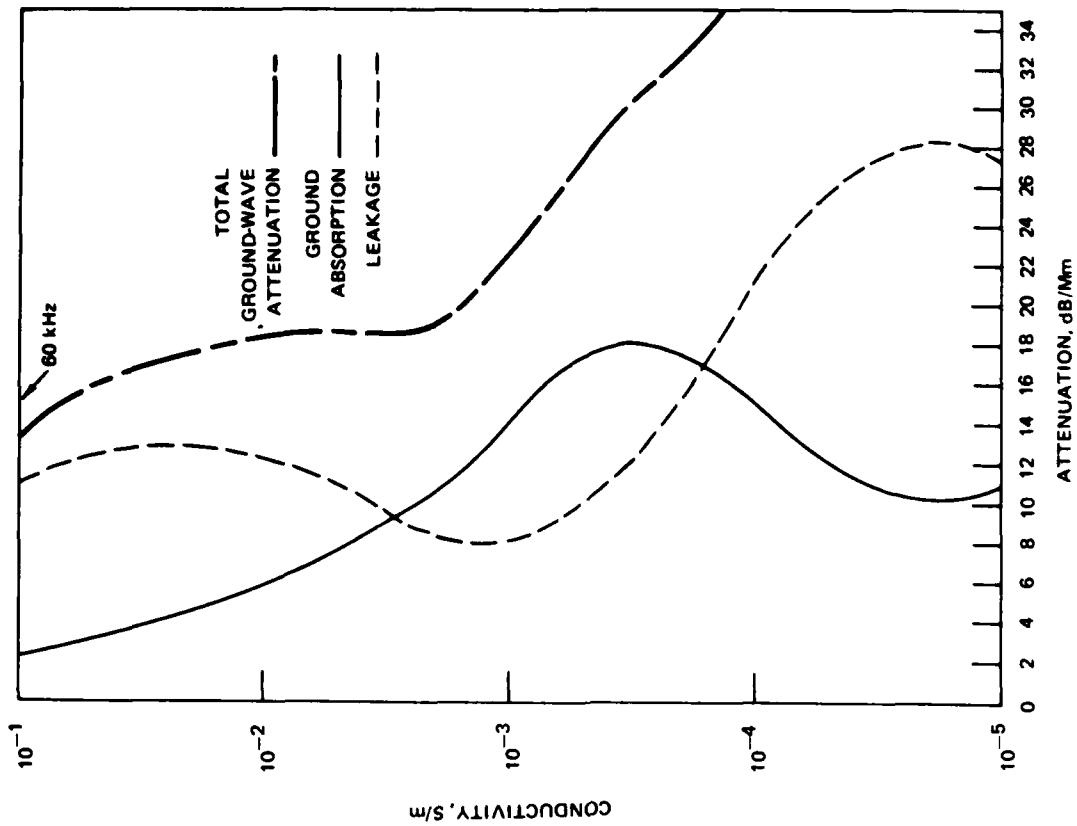


FIGURE 5d

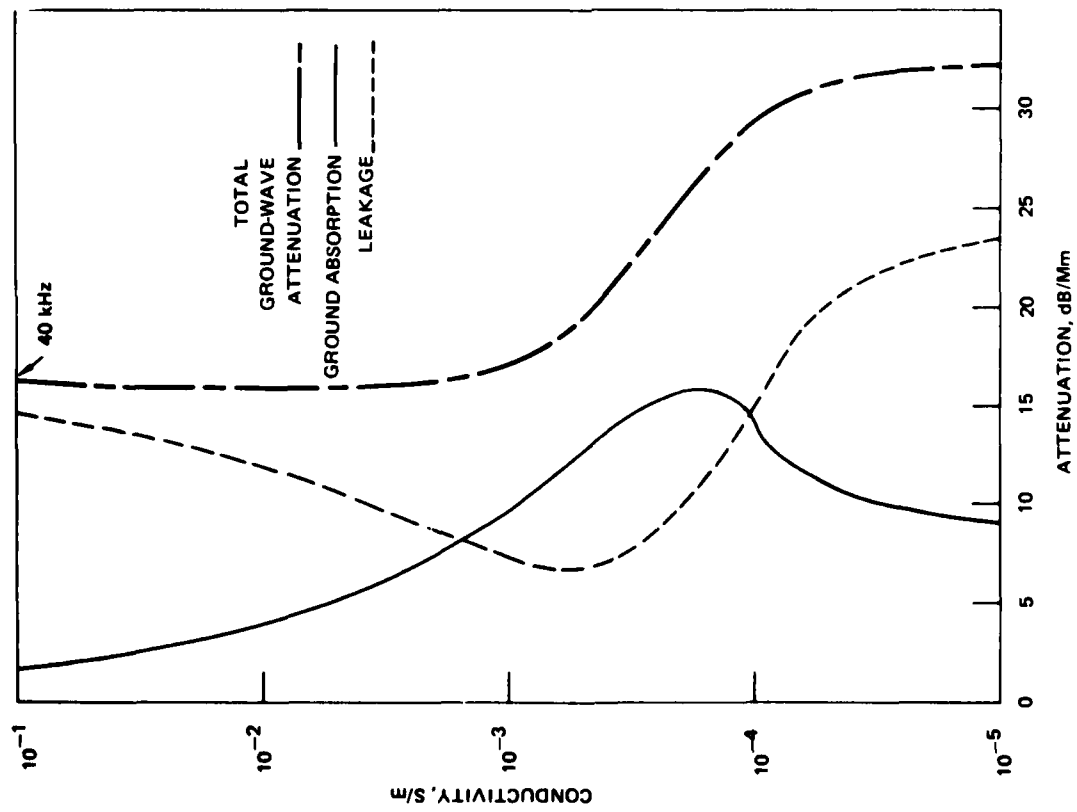


FIGURE 5c

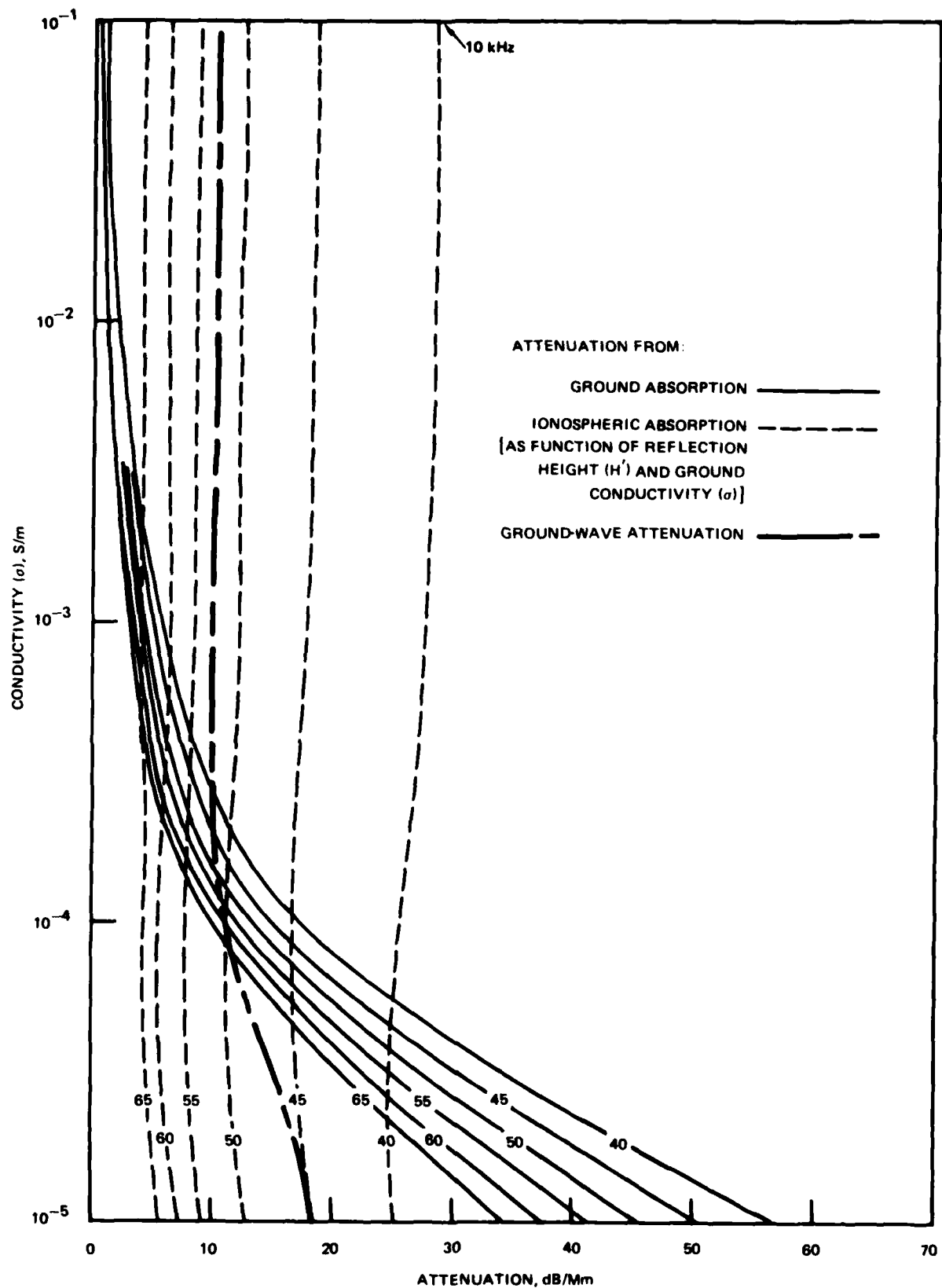


Figure 6 a-d. Attenuation rate of the principal waveguide mode resulting from ground absorption (solid curve) and resulting from ionospheric absorption (dashed curve) as a function of ground conductivity for a number of reflection heights H' . The broken curve is the ground-wave attenuation as a function of surface conductivity.

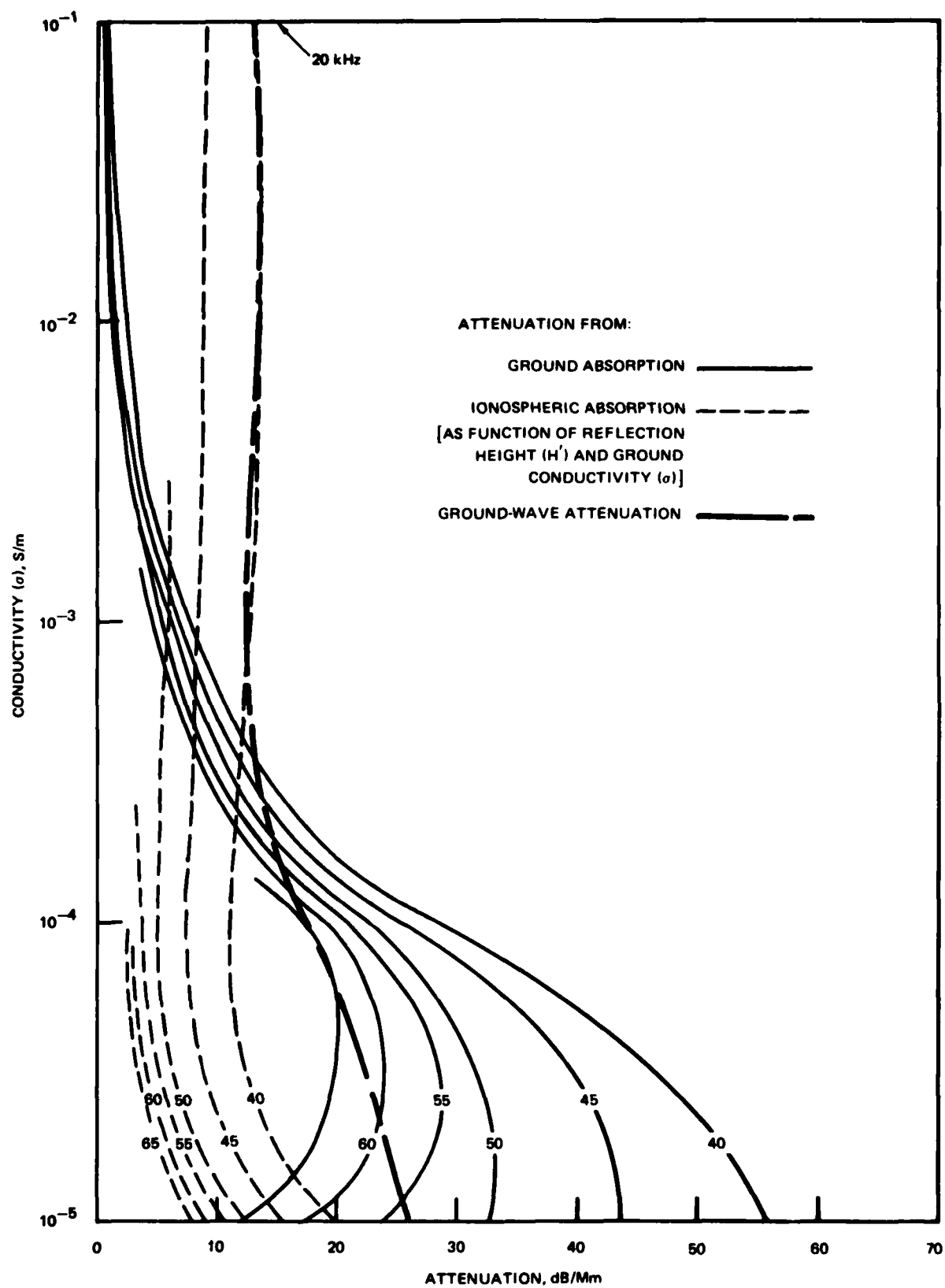


FIGURE 6b

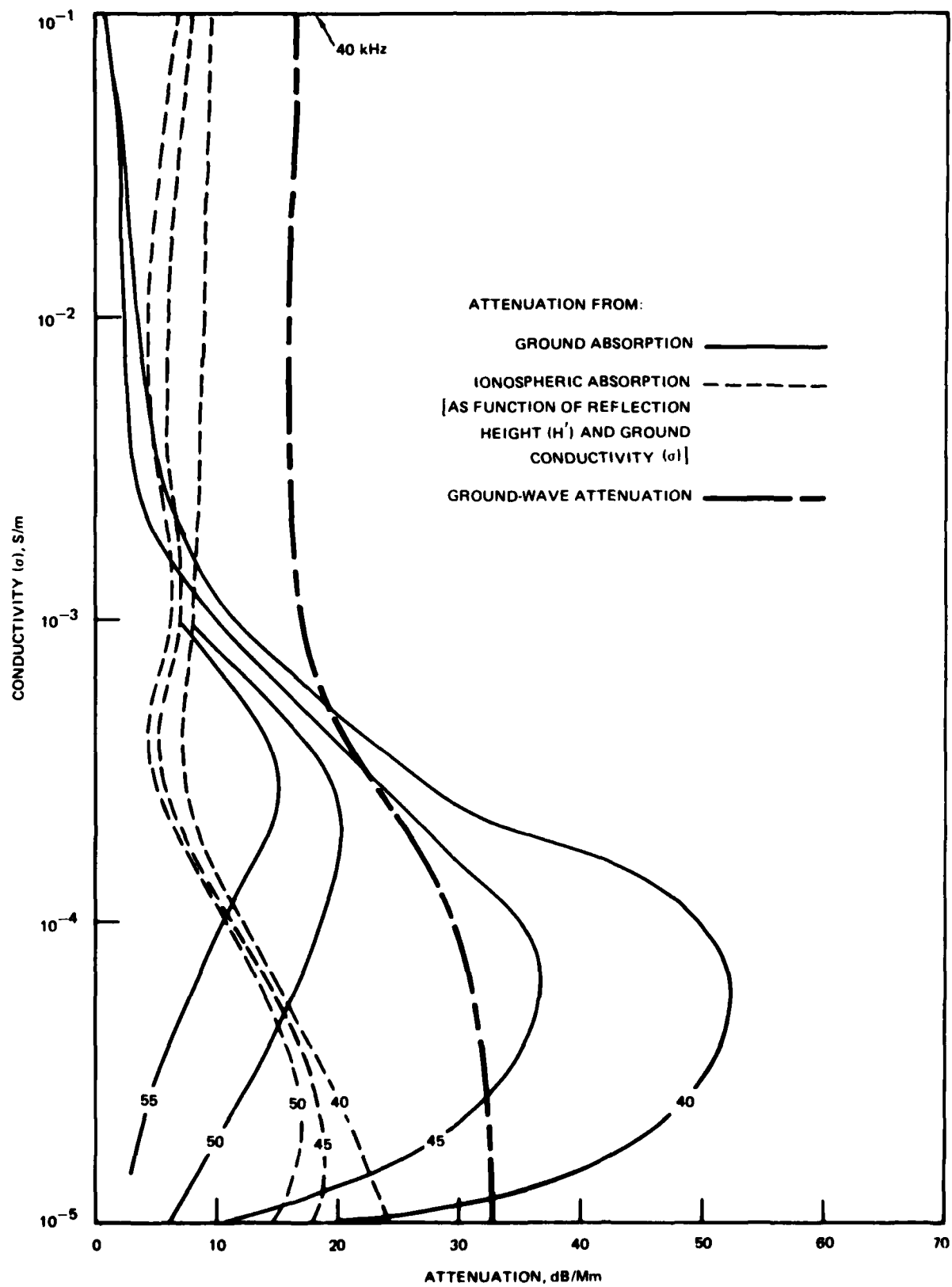


FIGURE 6c

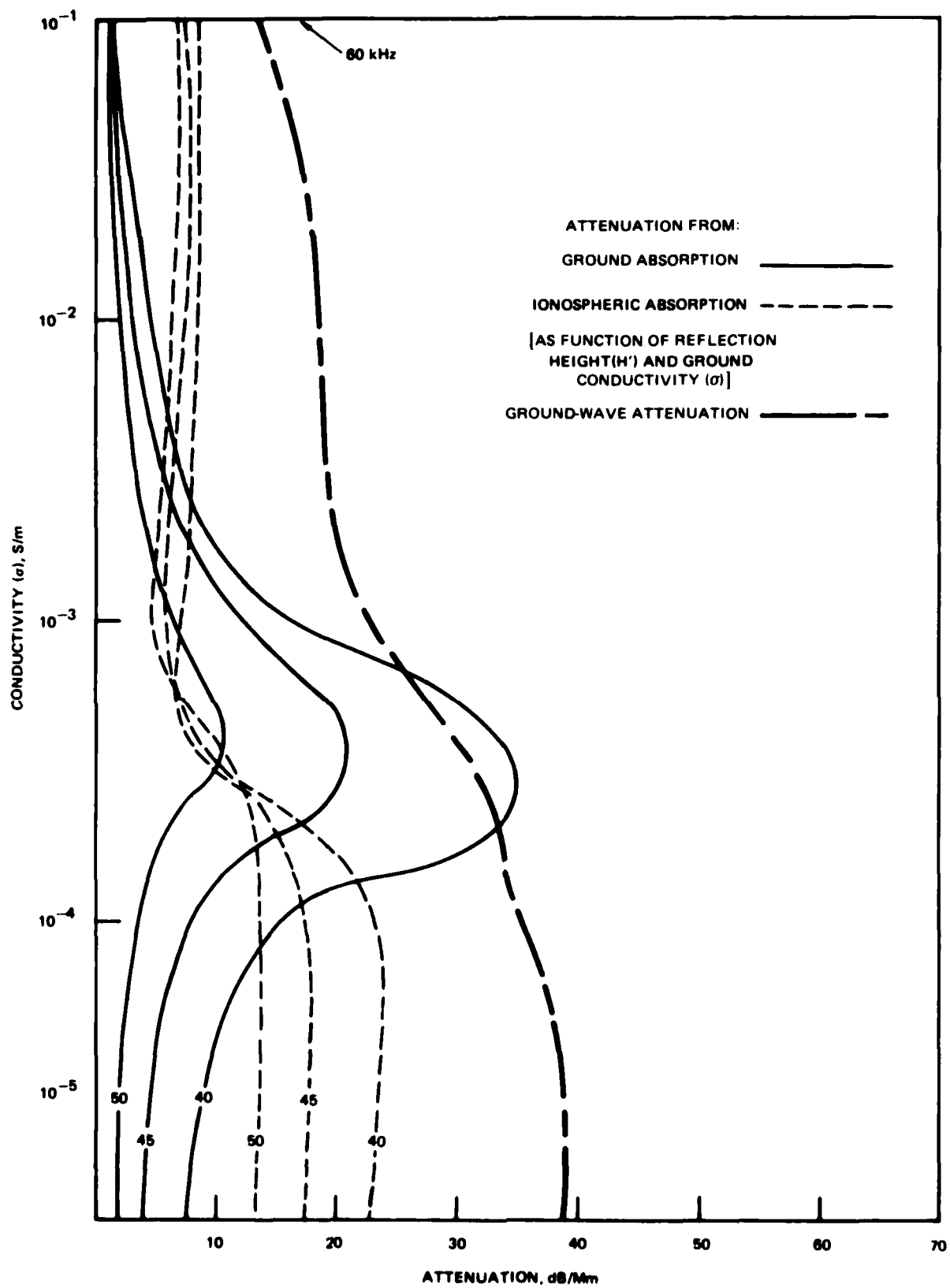


FIGURE 6d

3. DISCUSSION OF RESULTS

3.1 COMPARISON OF WAVEGUIDE AND GROUND WAVE

Waveguide mode attenuation rates were calculated over the frequency band of 10 to 60 GHz by using the NOSC-developed "MODESRCH"¹¹ program. Ground-wave attenuation rates were calculated by using an adaptation of a computer program developed by Berry and Herman.¹² Both programs also were used to calculate attenuation rates for a number of ground conductivities, but the waveguide calculations were also parametric in terms of the "reflection height" for exponential ionospheric profiles. The results of the calculations are shown in figures 7a through 7g, where the curves in each figure are for a specific ground conductivity. The conductivities range from 10^{-1} S/m (figure 7a) to 10^{-5} S/m (figure 7g). The attenuation rate for a mode which is characterized by a complex eigenangle at the ground equal to the Brewster angle is given by the curve labeled θ_B .

Ionospheric anisotropy was included in the waveguide mode calculations. All results are for a dip angle of 51° , a magnetic flux density of 4.31×10^{-5} webers per square meter, and a geomagnetic azimuth of propagation of 58.5° . However, because most of the calculations are for depressed daytime ionospheres, the magnetic effects are negligible and the results are representative of isotropic ionospheres.

From figures 7a-g, it is clear that path losses under depressed ionospheres can materially exceed the theoretical ground-wave losses, particularly at the low end of the vlf-lf spectrum. However, for surface conductivities equal to or greater than about 10^{-3} S/m, the ionosphere must be extraordinarily depressed before waveguide attenuation rates exceed ground-wave rates, particularly at lf.

At conductivities below 10^{-3} S/m, the waveguide attenuation rates begin to exceed ground-wave rates for moderately depressed ionospheres. In the 3×10^{-4} to 10^{-4} S/m conductivity range, the phenomenon pointed out by Westerlund and Reder⁷ becomes evident. That is, the maximum attenuation across the frequency band is closely associated with the modal eigenangles near the Brewster angle.

The data described by figures 7a-g are summarized from a different perspective in figure 8, where those combinations of reflection height H' and surface conductivity σ , which lie above each frequency curve, produce a smaller attenuation rate for the principal TM mode than the ground wave. For combinations of H' and σ lying below each frequency curve, the principal earth-ionosphere waveguide mode attenuation rate is greater than that of the ground wave.

11. Morfitt, D.G., and C.H. Shellman, 'MODESRCH', an Improved Computer Program for Obtaining ELF/VLF/LF Mode Constants in an Earth-Ionosphere Waveguide, Naval Electronics Laboratory Center Interim Report No. 77T for DNA, 1 October 1976.
12. Berry, L.A., and J.E. Herman, A Wave Hop Propagation Program for an Anisotropic Ionosphere, Telecommunications Research Report OT/ITS RR11, US Department of Commerce, Office of Telecommunications, Institute of Telecommunications Sciences, Boulder, CO, April 1971.

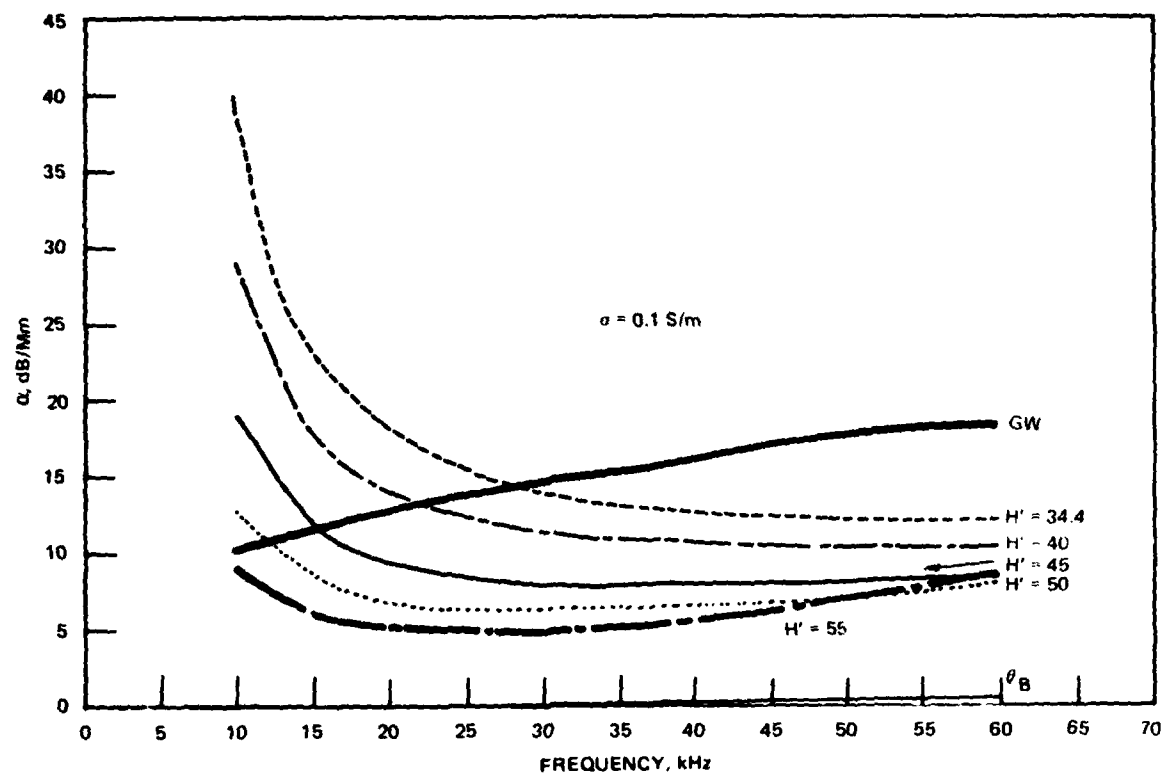


FIGURE 7a

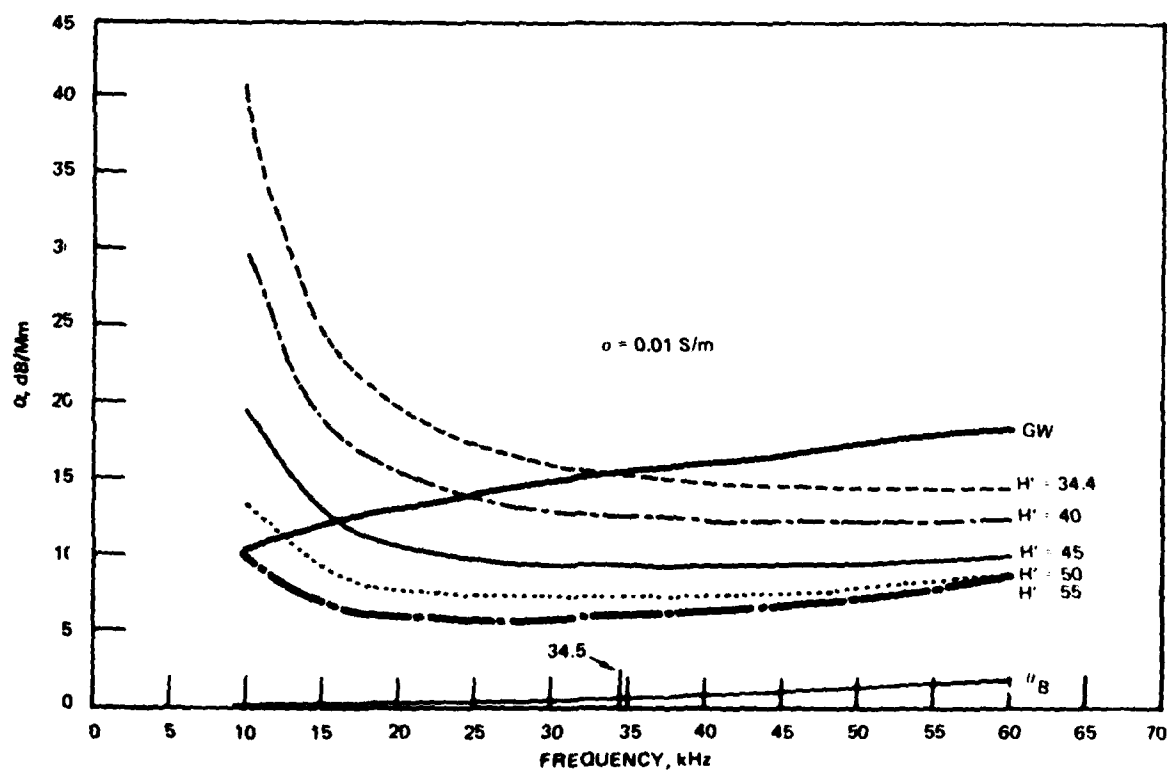


FIGURE 7b

Figure 7 a-g. Attenuation rate of the principal waveguide mode as a function of frequency for a number of reflection heights H' and for the ground conductivity σ specified on each figure. The ground-wave attenuation rate (curve GW) and the attenuation rate of a mode characterized by eigenangles equal to the complex Brewster angle (curve θ_B) are also shown for each ground conductivity.

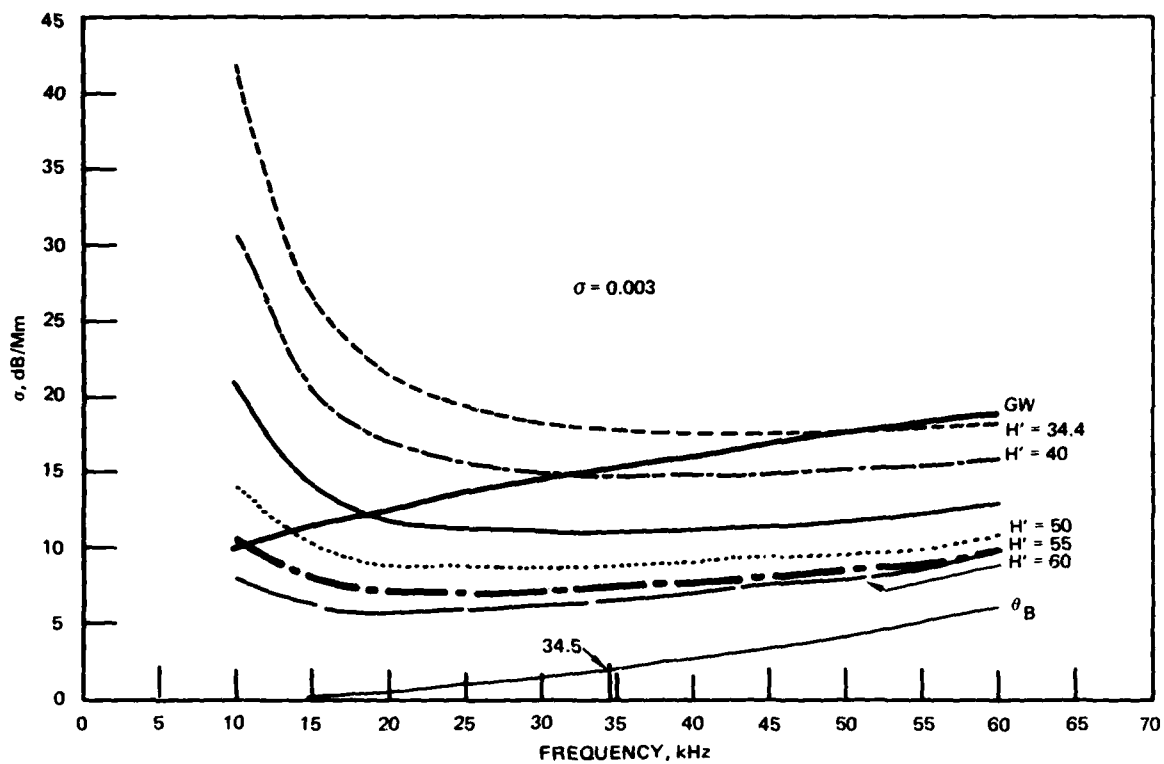


FIGURE 7c

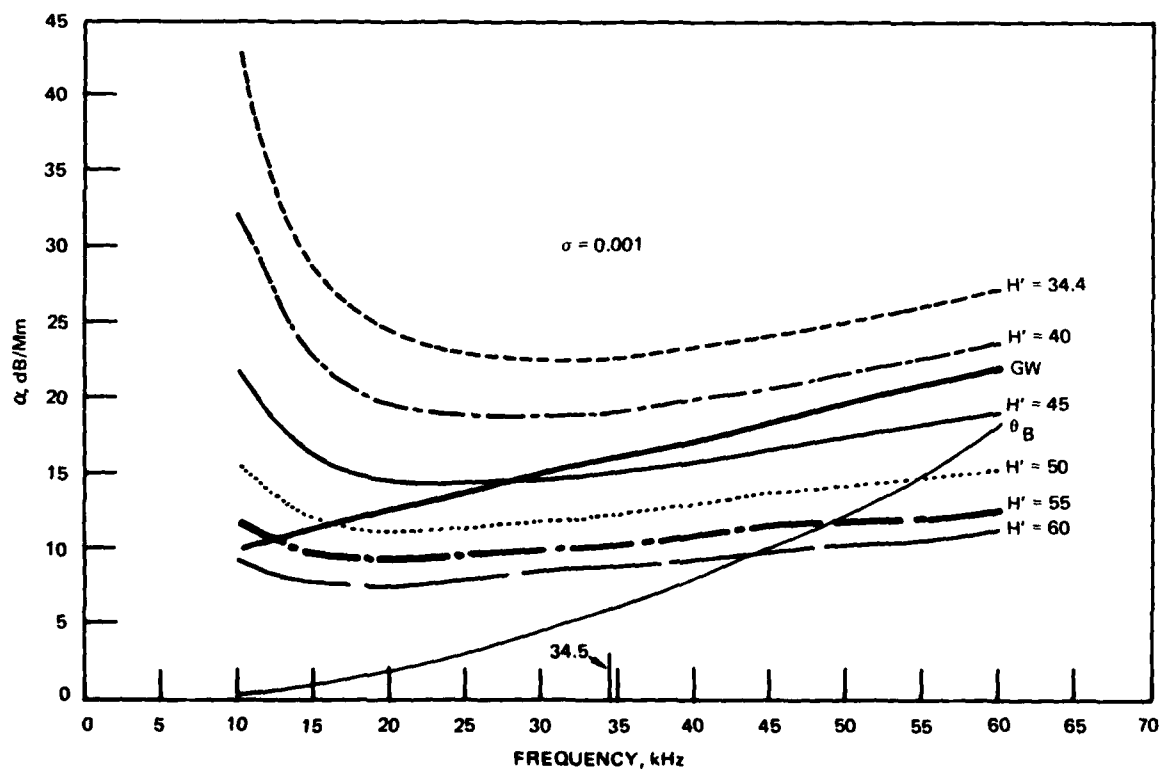


FIGURE 7d

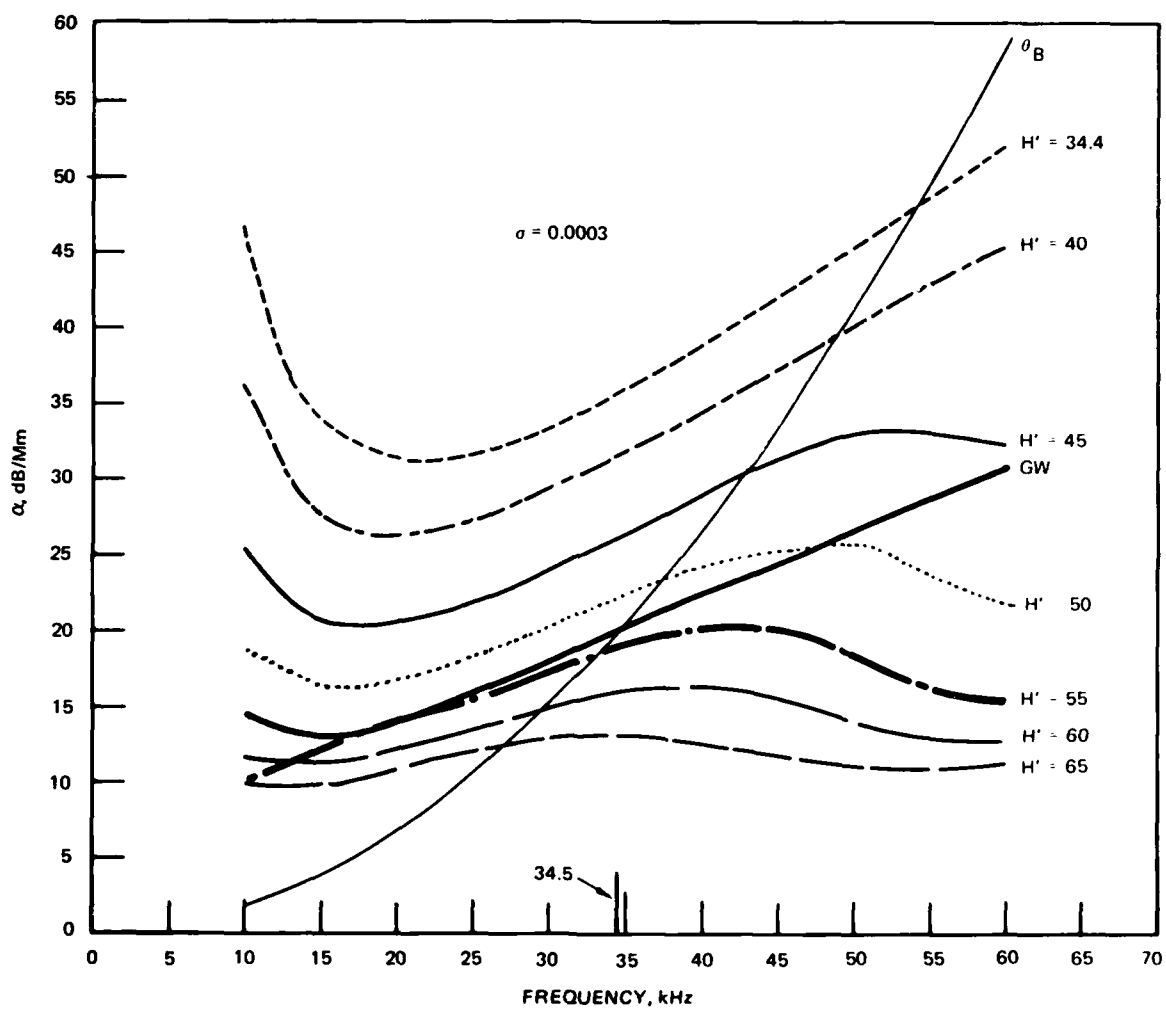


FIGURE 7e

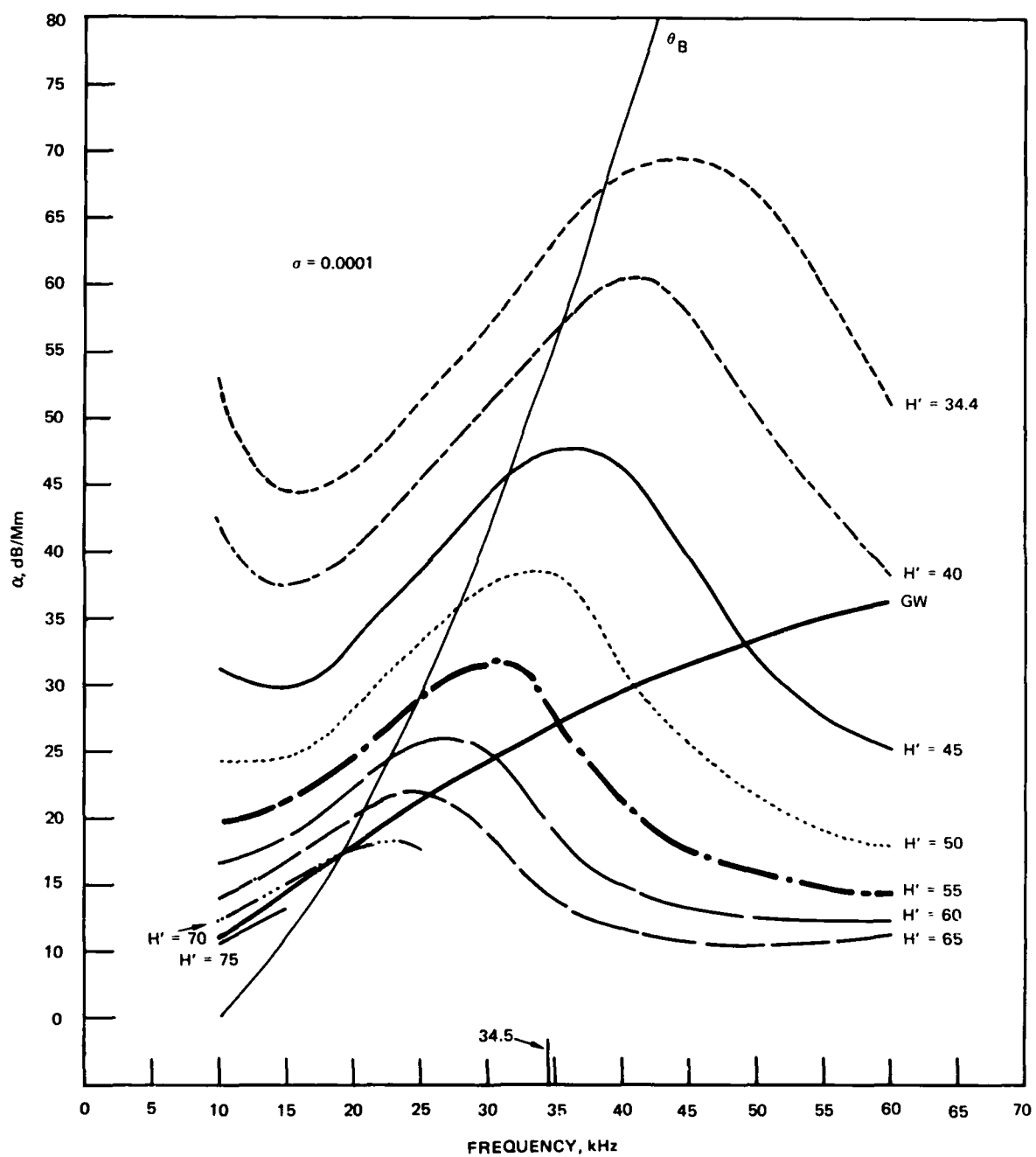


FIGURE 7f

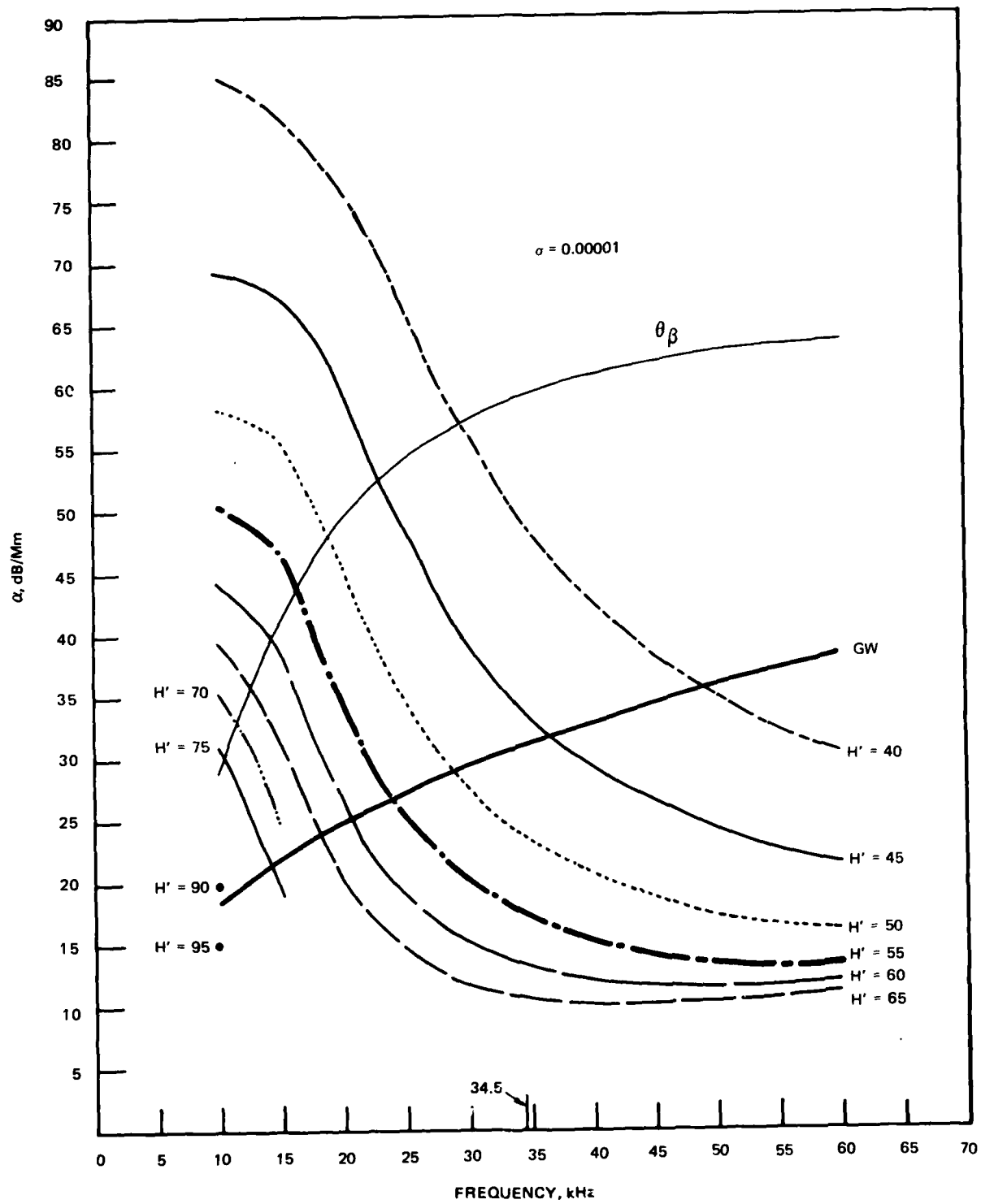


FIGURE 7g

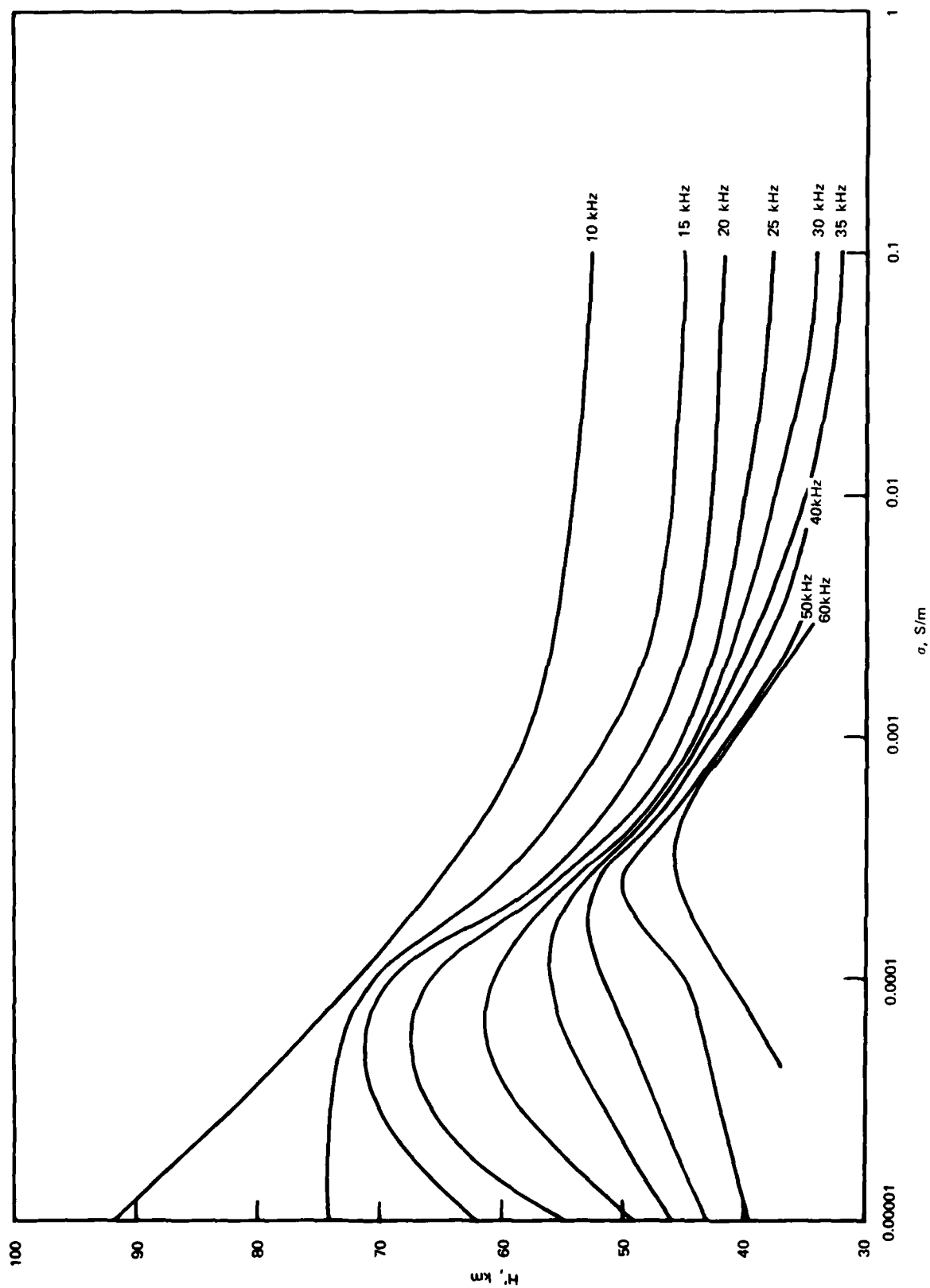


Figure 8. Combinations of reflection height H' and surface conductivity σ which produce a principal TM waveguide mode attenuation rate equal to the ground-wave attenuation rate. For those combinations of H' and σ lying above each of the frequency curves, the TM waveguide mode attenuation is less than the ground-wave attenuation rate for that frequency and ground conductivity. For combinations below the curve, the TM mode attenuation rate is greater than the ground-wave attenuation rate.

For the particular ionospheric conductivity gradient β used for this study and for ground conductivity σ less than about 10^{-3} S/m, ionospheric depressions typical of polar cap events or nuclear disturbances can produce path losses greater than ground-wave path losses. Although the conductivity gradient $\beta = 0.2515 \text{ km}^{-1}$ was selected after an examination of a number of conductivity profiles for variously disturbed ionospheres, it should be pointed out that the model becomes less appropriate for the more normal reflection heights. For example, figure 7g shows waveguide mode attenuation rates at 10 kHz for reflection heights up to 95 km. From the data, one deduces that for 10^{-5} S/m ground conductivity and reflection heights below 90 km, waveguide path losses exceed ground-wave path losses. But it is hard to imagine the circumstances which would produce a scale height $\beta = 0.2515 \text{ km}^{-1}$ for altitudes much greater than 70 km. Thus the results shown in figures 7 and 8 are most useful for locating possible problem areas but not their precise boundaries.

4. CONCLUSIONS AND RECOMMENDATIONS

The assumption that Lf communications systems designed to operate at ground-wave signal levels will maintain connectivity in a severe nuclear environment is safe only for propagation over relatively highly conductive ground. At the lower vlf frequencies, the assumption is never safe. Lf systems designed to operate on ground-wave propagation over highly conductive ground should have a considerable system margin. For Lf propagation over poorly conducting ground or fresh water ice, losses may considerably exceed ground-wave losses when the ionosphere is moderately depressed.

When the DNA working group recommended that Lf systems be designed on the basis of a surviving ground wave, it was recognized that methods for calculating Lf propagation and the propagation environment were inadequate. Today, although we still have questions regarding some of the air chemistry, there is little doubt that severe disturbances can be modeled with good confidence. In addition, we no longer rely on "wave-hop" methods (with the attendant inaccuracies for severely disturbed ionospheres) for calculating Lf propagation parameters. Waveguide mode propagation prediction methods work well to at least 100 kHz. Because of the possible errors and misconceptions which may arise from using the ground-wave computation for estimating Lf coverage in severely disturbed environments, it seems far safer to do a complete propagation analysis of coverage by means of numerical methods based on waveguide mode theory.

REFERENCES

1. Crain, C.M., An Overview Discussion of Propagation Effects of Nuclear Environments on VLF-LF Communications Systems, RAND Corporation Report to Defense Nuclear Agency, DNA 3778T, 31 August 1975.
2. Johler, J.R., Ground Wave Propagation in a Normal and an Ionized Atmosphere, ESSA Research Laboratories Report ERL 121-ITS 85, July 1969.
3. Johler, J.R., Atmospheric Nuclear Disturbances with Respect to the Ground Wave, ESSA Research Laboratories Technical Memorandum, ERLTM-ITS 217, March 1970.
4. Pappert, R.A., Effects of Elevation and Ground Conductivity on Horizontal Dipole Excitation of the Earth-Ionosphere Waveguide, Radio Science, vol 5, pp 579-590, March 1980.
5. Field, E.C., C. Greifinger, and K. Schwartz, Transpolar Propagation of Long Radio Waves, R-683-DASA, DASA 2621, RAND Corporation, March 1971.
6. Westerlund, S., F.H. Reder, and C. Abom, Effects of Polar Cap Absorption Events on VLF Transmissions, Planetary and Space Science, 17, pp 1329-1374, 1969.
7. Westerlund, S., and F.H. Reder, VLF Radio Signals Propagating over the Greenland Ice-Sheet, Journal of Atmospheric and Terrestrial Physics, vol 35, pp 1475-1491, 1973.
8. Wait, J.R., and K.P. Spies, Characteristics of the Earth-Ionosphere Waveguide for VLF Radio Waves, US Dept of Commerce, National Bureau of Standards, Technical Note 300.
9. Budden, K.G., The Waveguide Mode Theory of Wave Propagation, Logos Press, London, 1961.
10. Booker, H.G., and W. Walkinshaw, The Mode Theory of Tropospheric Refraction and its Relation to Wave-Guides and Diffraction, in Report: Meteorological Factors in Radio Wave Propagation, pp 80-127, London, Physical Society, 1946.
11. Morfitt, D.G., and C.H. Shellman, 'MODESRCH', an Improved Computer Program for Obtaining ELF/VLF/LF Mode Constants in an Earth-Ionosphere Waveguide, Naval Electronics Laboratory Center Interim Report No. 77T for DNA, 1 October 1976.
12. Berry, L.A., and J.E. Herman, A Wave Hop Propagation Program for an Anisotropic Ionosphere, Telecommunications Research Report OT/ITS RR11, US Department of Commerce, Office of Telecommunications, Institute of Telecommunications Sciences, Boulder, CO, April 1971.

DISTRIBUTION LIST

DEPARTMENT OF DEFENSE
ASSISTANT SECRETARY OF DEFENSE
CMD, CONT, COMM & INTELL
DEPARTMENT OF DEFENSE
WASHINGTON, DC 20301
M EPSTEIN
J BABCOCK

DIRECTOR
COMMAND CONTROL TECHNICAL CENTER
11440 ISAAC NEWTON SQUARE, N
RESTON, VA 22091
C-650

DIRECTOR
COMMAND CONTROL TECHNICAL CENTER
ROOM ME682, THE PENTAGON
WASHINGTON, DC 20301
C-312

DIRECTOR
DEFENSE ADVANCED RESEARCH PROJECT
AGENCY
1400 WILSON BLVD
ARLINGTON, VA 22209
NUCLEAR MONITORING RSCH
STRATEGIC TECH OFFICE

DEFENSE COMMUNICATION ENGINEERING CENTER
1860 WIEHLE AVENUE
RESTON, VA 22090
CODE R220 (M HOROWITZ)
CODE R720 (JOHN WORTHINGTON)
CODE R410 (JAMES W McLEAN)
CODE R103

DIRECTOR
DEFENSE COMMUNICATIONS AGENCY
WASHINGTON, DC 20305
CODE 810 (RW ROSTRON)
CODE 480
CODE 1018 (MAJ ROOD)

DEFENSE COMMUNICATIONS AGENCY
WWMCCS SYSTEM ENGINEERING ORG
WASHINGTON, DC 20305
RL CRAWFORD

DEFENSE TECHNICAL INFORMATION CENTER
CAMERON STATION
ALEXANDRIA, VA 22314
TC (12)

DIRECTOR
DEFENSE INTELLIGENCE AGENCY
WASHINGTON, DC 20301
DIAST-5
DIAAP (ALBERT L WISE)
DB-4C (EDWARD OFARRELL)

DIRECTOR
DEFENSE NUCLEAR AGENCY
WASHINGTON, DC 20305
DDST
TISI ARCHIVES
TITL TECH LIBRARY (3)
RAAE (3)
STVL

COMMANDER
FIELD COMMAND
DEFENSE NUCLEAR AGENCY
KIRTLAND AFB, NM 87115
FCPR

DIRECTOR
INTERSERVICE NUCLEAR WEAPONS SCHOOL
KIRTLAND AFB, NM 87115
DOCUMENT CONTROL

DIRECTOR
JOINT STRAT TGT PLANNING STAFF JCS
OFFUTT AFB
OMAHA, NB 68113
JPST (CAPT DG GOETZ)

CHIEF
LIVERMORE DIVISION FLD COMMAND DNA
LAWRENCE LIVERMORE LABORATORY
PO BOX 808
LIVERMORE, CA 94550
FCPRL

DIRECTOR
NATIONAL SECURITY AGENCY
FT GEORGE G MEADE, MD 20755
W65
OLIVER H BARTLETT W32
TECHNICAL LIBRARY
JOHN SKILLMAN R52

OJCS/J-3
THE PENTAGON
WASHINGTON, DC 20301
OPERATIONS (WWMCCS EVAL
OFF, MR TOMA)

OJCS/J-5
THE PENTAGON
WASHINGTON, DC 20301
PLANS & POLICY (NUCLEAR DIVISION)

UNDER SECY OF DEFENSE FOR RESEARCH
AND ENGINEERING
DEPARTMENT OF DEFENSE
WASHINGTON, DC 2-301
S&SS (OS)

DEPARTMENT OF THE ARMY
COMMANDER/DIRECTOR
ATMOSPHERIC SCIENCES LABORATORY
US ARMY ELECTRONICS COMMAND
WHITE SANDS MISSILE RANGE, NM 88002
DELAS-AE-M (FE NILES)

COMMANDER
HARRY DIAMOND LABORATORIES
2800 POWDER MILL RD
ADELPHI, MD 20783
DELHD-NP (FRANCIES N WIMENITZ)
MILDRED H WEINER DRXDO-II

COMMANDER
US ARMY ELECTRONICS RESEARCH &
DEVELOPMENT COMMAND
FORT MONMOUTH, NJ 07703
DRSEL-RD
(JE QUIGLEY)

COMMANDER
US ARMY FOREIGN SCIENCE & TECH CENTER
220 7TH STREET, NE
CHALOTTESVILLE, VA 22901
R JONES
PA CROWLEY

COMMANDER
US ARMY NUCLEAR AGENCY
7500 BACKLICK ROAD
BUILDING 2073
SPRINGFIELD, VA 22150
MONA-WE (J BERBERET)

CHIEF
US ARMY RESEARCH OFFICE
PO BOX 12211
TRIANGLE PARK, NC 27709
DRXRD-ZC

DEPARTMENT OF THE NAVY
CHIEF OF NAVAL OPERATIONS
NAVY DEPARTMENT
WASHINGTON, DC 20350
OP 941
OP-604C3
OP 943 (LCDR HUFF)
OP 981

CHIEF OF NAVAL RESEARCH
NAVY DEPARTMENT
ARLINGTON, VA 22217
CODE 402
CODE 420
CODE 421
CODE 461
CODE 464

COMMANDING OFFICER
NAVAL INTELLIGENCE SUPPORT CENTER
4301 SUITLAND RD BLDG 5
WASHINGTON, DC 20390

COMMANDER
NAVAL OCEAN SYSTEMS CENTER
SAN DIEGO, CA 92152
CODE 81 (HD SMITH)
CODE 532 (3)
CODE 532 (WILLIAM F MOLER)

COMMANDING OFFICER
NAVAL RESEARCH LABORATORY
WASHINGTON, DC 20375
CODE 5410 (JOHN DAVIS)
CODE 7701 (JACK D BROWN)
CODE 5461 TRANS IONO PROP
CODE 5465 PROP APPLICATIONS
CODE 5460 ELECTROMAG PROP BR
CODE 2600 TECH LIBRARY (2)

OFFICER-IN-CHARGE
WHITE OAK LABORATORY
NAVAL SURFACE WEAPONS CENTER
SILVER SPRING, MD 20910
CODE WA501 NAVY NUC PRGMS OFF
CODE WX21 TECH LIBRARY

COMMANDER
NAVAL TELECOMMUNICATIONS COMMAND
NAVTELCOM HEADQUARTERS
4401 MASSACHUSETTS AVE, NW
WASHINGTON, DC 20390
CODE 24C

COMMANDING OFFICER
NAVY UNDERWATER SOUND LABORATORY
FORT TRUMBULL
NEW LONDON, CT 06320
PETER BANNISTER
DA MILLER

DIRECTOR
STRATEGIC SYSTEMS PROJECT OFFICE
NAVY DEPARTMENT
WASHINGTON, DC 20376
NSP-2141

DEPARTMENT OF THE AIR FORCE
COMMANDER
ADC/DC
ENT AFB, CO 80912
DC (MR LONG)

COMMANDER
ADCOM/XPD
ENT AFB, CO 80912
XPQDQ
XP

AF GEOPHYSICS LABORATORY, AFSC
HASCAM AFB, MA 01731
CRU (S HOROWITZ)
PHP (JULES AARONS)
OPR (JAMES C ULWICK)
OPR (ALVA T STAIR)
SUOL (RESEARCH LIBRARY) (2)

AF WEAPONS LABORATORY, AFSC
KIRTLAND AFB, NM 87117
SUL (2)
SAS (JOHN M KAMM)
DYC (CAPT L WITTWER)

AFTAC
PATRICK AFB, FL 32925
TN
TD-3
TD-5
TF/MAJ WILEY

AIR FORCE AVIONICS LABORATORY, AFSC
WRIGHT-PATTERSON AFB, OH 45433
AAD

COMMANDER
FOREIGN TECHNOLOGY DIVISION, AFSC
WRIGHT-PATTERSON AFB, OH 45433
ETD BL BALLARD

HQ USAF/RD
WASHINGTON, DC 20330
RDQ

HEADQUARTERS
NORTH AMERICAN AIR DEFENSE COMMAND
1500 EAST BOULDER
COLORADO SPRINGS, CO 80912
CHIEF SCIENTIST

COMMANDER
ROME AIR DEVELOPMENT CENTER, AFSC
GRIFFISS AFB, NY 13440
EMTLD DOC LIBRARY

COMMANDER
ROME AIR DEVELOPMENT CENTER, AFSC
HANSCOM AFB, MA 01731
EEP JOHN RASMUSSEN

SAMSO/MN
NORTON AFB, CA 92409
MINUTEMAN (NMML LTC KENNEDY)

COMMANDER IN CHIEF
STRATEGIC AIR COMMAND
OFFUTT AFB, NB 68113
NRT
XPFS (MAJ BRIAN G STEPHAN)
DOK (CHIEF SCIENTIST)

US ENERGY RESEARCH AND DEV ADMIN
DEPARTMENT OF ENERGY
ALBUQUERQUE OPERATIONS OFFICE
PO BOX 5400
ALBUQUERQUE, NM 87115
DOC CON FOR D W SHERWOOD

DIVISION OF MILITARY APPLICATION
DEPARTMENT OF ENERGY
WASHINGTON, DC 20545
DOC CON FOR DONALD I GALE

LAWRENCE LIVERMORE LABORATORY
PO BOX 808
LIVERMORE, CA 94550
GLENN C WERTH L-216
TECH INFO DEPT L-3

LOS ALAMOS SCIENTIFIC LABORATORY
PO BOX 1663
LOS ALAMOS, NM 87545
DOC CON FOR T F TASCHER
DOC CON FOR D R WESTERVELT
DOC CON FOR P W KEATON
DOC CON FOR J H COON

SANDIA LABORATORIES
LIVERMORE LABORATORY
PO BOX 969
LIVERMORE, CA 94550
DOC CON FOR B E MURPHEY
DOC CON FOR T B COOK ORG 8000

SANDIA LABORATORIES
PO BOX 5800
ALBUQUERQUE, NM 87115
DOC CON FOR SPACE PROJ DIV
DOC CON FOR A D THORNBROUGH, ORG 1245
DOC CON FOR W C MYRA
DOC CON FOR 3141 SANDIA RPT COLL

OTHER GOVERNMENT
DEPARTMENT OF COMMERCE
NATIONAL BUREAU OF STANDARDS
WASHINGTON, DC 20234
RAYMOND T MOORE

DEPARTMENT OF COMMERCE
OFFICE OF TELECOMMUNICATIONS
INSTITUTE FOR TELCOM SCIENCE
BOULDER, CO 80302
WILLIAM F UTLAUT
L A BERRY
A GLENN JEAN
D D CROMBIE
J R WAIT

DEPARTMENT OF TRANSPORTATION
OFFICE OF THE SECRETARY
TAD-44.1, ROOM 10402-B
400 7TH STREET, SW
WASHINGTON, DC 20590
R L LEWIS
R H DOHERTY

DEPARTMENT OF DEFENSE CONTRACTORS
AEROSPACE CORPORATION
PO BOX 92957
LOS ANGELES, CA 90009
IRVING M GARFUNKEL

ANALYTICAL SYSTEMS ENGINEERING CORP
5 OLD CONCORD RD
BURLINGTON, MA 01803
RADIO SCIENCES

THE BOEING COMPANY
PO BOX 3707
SEATTLE, WA 98124
GLENN A HALL
J F KENNEY

UNIVERSITY OF CALIFORNIA
AT SAN DIEGO
MARINE PHYSICAL LAB OF THE
SCRIPPS INSTITUTE OF OCEANOGRAPHY
SAN DIEGO, CA 92132
HENRY G BOOKER

COMPUTER SCIENCES CORPORATION
PO BOX 530
6565 ARLINGTON BLVD
FALLS CHURCH, VA 22046
D BLUMBERG

UNIVERSITY OF DENVER
COLORADO SEMINARY
DENVER RESEARCH INSTITUTE
PO BOX 10127
DENVER, CO 80210
DONALD DUBBERT
HERBERT REND

ESL, INC
495 JAVA DRIVE
SUNNYVALE, CA 94086
JAMES MARSHALL

GENERAL ELECTRIC COMPANY
SPACE DIVISION
VALLEY FORGE SPACE CENTER
GODDARD BLVD KING OF PRUSSIA
PO BOX 8555
PHILADELPHIA, PA 19101
SPACE SCIENCE LAB (MH BORTNER)

GENERAL ELECTRIC COMPANY
TEMPO-CENTER FOR ADVANCED STUDIES
816 STATE STREET
PO DRAWER QQ
SANTA BARBARA, CA 93102
B GAMBILL
DASIAC (2)
DON CHANDLER
WARREN S KNAPP

GEOPHYSICAL INSTITUTE
UNIVERSITY OF ALASKA
FAIRBANKS, AK 99701
T N DAVIS
NEAL BROWN
TECHNICAL LABORATORY

GTE SYLVANIA, INC
ELECTRONICS SYSTEMS GRP
EASTERN DIVISION
77 A STREET
NEEDHAM, MA 02194
MARSHAL CROSS

IIT RESEARCH INSTITUTE
10 WEST 35TH STREET
CHICAGO, IL 60616
TECHNICAL LIBRARY

UNIVERSITY OF ILLINOIS
DEPARTMENT OF ELECTRICAL ENGINEERING
URBANA, IL 61803
AERONOMY LABORATORY (2)

JOHNS HOPKINS UNIVERSITY
APPLIED PHYSICS LABORATORY
JOHNS HOPKINS ROAD
LAUREL, MD 20810
J NEWLAND
PT KOMISKE

LOCKHEED MISSILES & SPACE CO, INC.
3251 HANOVER STREET
PALO ALTO, CA 94304
E E GAINES
W L IMHOF D/52-12
J B REAGAN D652-12
R G JOHNSON D/52-12

LOWEL RESEARCH FOUNDATION
450 AIKEN STREET
LOWELL, MA 01854
DR BIBL

MASSACHUSETTS INSTITUTE OF TECHNOLOGY
LINCOLN LABORATORY
PO BOX 73
LEXINGTON, MA 02173
DAVE WHITE
J H PANNELL L-246
D M TOWLE

MISSION RESEARCH CORPORATION
735 STATE STREET
SANTA BARBARA, CA 93101
R HENDRICK
F FAJEN
M SCHEIBE
J GILBERT
C L LONGMIRE

MITRE CORPORATION
PO BOX 208
BEDFORD, MA 01730
G HARDING

PACIFIC-SIERRA RESEARCH CORP
1456 CLOVERFIELD BLVD
SANTA MONICA, CA 90404
E C FIELD, JR

PENNSYLVANIA STATE UNIVERSITY
IONOSPHERIC RESEARCH LABORATORY
318 ELECTRICAL ENGINEERING EAST
UNIVERSITY PARK, PA 16802
IONOSPHERIC RSCH LAB (2)

R&D ASSOCIATES
PO BOX 9695
MARINA DEL REY, CA 90291
FORREST GILMORE
WILLIAM J KARZAS
PHYLLIS GREIFINGER
CARL GREIFINGER
A ORY
BRYAN GABBARD
R P TURCO
SAUL ALTSCHULER

RAND CORPORATION
1700 MAIN STREET
SANTA MONICA, CA 90406
TECHNICAL LIBRARY (2)
CULLEN CRAIN

SRI INTERNATIONAL
333 RAVENSWOOD AVENUE
MENLO PARK, CA 94025
DONALD NEILSON
GEORGE CARPENTER
W G CHETNUT
J R PETERSON
GARY PRICE

STANFORD UNIVERSITY
RADIO SCIENCE LABORATORY
STANFORD, CA 94305
R A HELLIWELL
FRASER SMITH
J KATSUFRAKIS

TRW DEFENSE & SPACE SYS GROUP
ONE SPACE PARK
REDONDO BEACH, CA 90278
DIANA DEE

CALIFORNIA INSTITUTE OF TECHNOLOGY
JET PROPULSION LABORATORY
4800 OAK GROVE DRIVE
PASADENA, CA 91103
ERNEST K SMITH
(MAIL CODE 144 B13)